The Tire Stacking Machine

Engineering Proposal

AER201 - Engineering Design
Professor M. Reza Emami
TA: Geoff Donoghue
Team 27

Bipasha Goyal - 1004532222
Yewon Lee - 1004407260
Yuqian Zhou - 1003234289

Division of Engineering Science
University of Toronto

January 30th 2019

TABLE OF CONTENTS

1 EXECUTIVE SUMMARY **4**

2 DEFINITIONS **4**

3 INTRODUCTION **5**

3.1 PROBLEM FORMULATION AND GOAL 5

3.2 OBJECTIVES 6

3.3 METRICS 6

3.4 CONSTRAINTS 10

3.5 FUNCTIONAL ANALYSIS 10

3.6 SURVEY 11

3.6.1 Literature Survey 11

3.6.2 Idea Survey 12

AER201 Tire Stacking Machine (2011, Champion) 12

AER201 Project (2011, Team 56) 13

US3955491A - Automotive Tire Stacking and Strapping Machine 13

3.6.3 Market Survey 14

US6527499B2: Automated tire loading/unloading and compression system 14

US5562392A: Tire-stacking device and accessories for use in cooperative arrangement with a lift truck 14

4 CONCEPTUALISATION **16**

4.1 SUBMODULE BREAKDOWN 16

4.1.1 Path of movement 16

4.2 ALTERNATIVE SOLUTIONS 17

4.2.1 Submodule 1: Stacking and unstacking mechanism 17

Tube and hook system 17

Pulley-weight system 19

Self-weight system 20

Vending machine mechanism 20

4.2.2 Submodule 2: Deployment mechanism 22

Tube and hook system See 4.2.1 for details. 22

Conveyor belt system 22

Trap door 22

Forklift 23

4.2.3 Submodule 3: Extension mechanism 23

4.2.4 Submodule 4: Sensors 24

4.2.5 Submodule : Microcontroller and development board 24

4.2.6 Alternative systematic designs 24
4.3 DECISION MAKING 24
4.3.1 Testing Protocol and Results 24
4.3.2 Analytical Hierarchy Process 26
4.3.2.1 Relative Preference and Relative Importance Matrices 27
RP Matrices for Stacking Mechanism 27
Consistency Check 30
Final Decision 30
4.3.3 Utility Based Decision Making 31
4.4 SPECIFICATION 32
4.4.1 Electromechanical Design 32
Design Overview 32
Tire Advancement and Deployment System 33
Extension System 36
Sensors' Location 37
Driving Mechanism 38
Specification of Motors 38
Wheels 40
4.4.2 Circuit Design 41
Motors 41
Sensors 44
Pole Detection Indicator Circuit 45
Power Supply and Step Down Circuits 45
4.4.3 Microcontroller Design 47
Pin assignment 47
Main program 49
5 PROJECT MANAGEMENT 50
5.1 STATEMENT OF WORK 50
Electromechanical Engineer 50
Electrical Engineer 50
Microcontroller Engineer 50
5.2 GANTT CHART 50
5.3 PERT CHART 50
5.4 BUDGETING 51
6 CONCLUSION 52
7. REFERENCES 54
8 APPENDICES 56

8.1 NUMERICAL DATA FROM ULTRASONIC SENSOR TEST 56
8.2 AHP FOR REMAINING SUBSYSTEMS 57
8.3 CALCULATIONS FOR MOTOR SELECTION 63
8.3.1 Differential Driving 63
Torque 63
RPM or Angular Velocity 63
8.3.2 Tire Advancer 64
RPM or Angular Velocity 64
Torque 64
8.3.3 Tube Extender 64
RPM or Angular Velocity 64
Torque 65
8.4 DATA SHEETS FOR MOTORS 65
8.5 DATA SHEETS FOR SENSORS 68
8.6 DATA SHEETS FOR MICROCONTROLLERS 72
8.7 DATA SHEETS FOR DRIVER BOARD 73
8.8 DATA SHEETS FOR ELECTRICAL COMPONENTS 74

1 EXECUTIVE SUMMARY

This project proposal puts forth a solution to the problem of deploying tires onto a series of poles. The position of the poles are semi-random, with varying distances between each consecutive poles and varying deviations of a pole's position with respect to an imaginary, vertical line on the floor.

The proposed solution consists of two tubes of square cross-section with a guiding rod within it, for the deployment of tires onto poles. The rod is straight inside the tubes, but forms a hook-like shape at the open end of both tubes. Tires are pushed towards the open end by increments of 2.7 cm at a time, to push one tire at a time towards the hook so that it slides down the hook and onto the pole. The deviations of a pole's position with respect to the imaginary line are accounted for through the tubes' extension mechanism, whereby the tubes can slide outwards to meet the position of the poles.

The machine will presented at the AER201 Engineering Design Competition 2019. The time required to prepare the machine will be 5 minutes, and the total operation of deploying tires (which will be known on the day of the competition) is expected to take less than 3 minutes. The funding requirements to build this machine is around $230 which accounts for the machine's material cost.

Yuqian Zhou, Yewon Lee, and Bipasha Goyal are the three members of this engineering design team. Yuqian is responsible for processing and control systems and will be developing the software for the solution. Yewon is responsible for the electromechanical subsystem, and will be constructing the prototype of the solution and incorporating its actuators. Bipasha is responsible for instrumentation and interfacing and will construct the digital and analog interfacing electronics to connect sensors and actuators to the microcontroller board. All three members will take active part in the integration of the three subsystems.

2 DEFINITIONS

In this section a few terms that are commonly used in the proposal are defined for clarification:
Machine: The scaled-down prototype of the autonomous tire stacking mobile platform
Tires: Toy truck tires used as scaled-down prototype for real tires
Operation: The setup created by the client on the day of testing
Desired Operation: The minimum operation the team requires the machine to complete
Stacking/Unstacking mechanism or storage: Storage of tires on machine
Deployment: Process of putting tires on poles

3 INTRODUCTION

3.1 PROBLEM FORMULATION AND GOAL

This proposal documents the design process towards a potential solution to the need presented by a tire manufacturing company for creating an autonomous tire stacking machine using mobile platforms. The conceptualised design is a scaled down, proof-of-concept prototype of a mobile platform that can travel along a row of poles and stack a desired number of tires on them.

The setup and required operation for a trial run of tire deployment is as follows:

- There will be anywhere between four and ten poles located along a line with a variance of 5 cm from the line. The poles have two parts to them - a wider base made of a box containing white sand granules and a black metal pole lodged through the center of the base. The overall height of the poles will be 19.5 ± 0.5 cm. The poles will have anywhere between zero to two tires stacked on them.
- The “tires” are toy truck rubber tires weighing 18 ± 3 g with 2.7 ± 0.2 cm thickness and inner and outer diameters of 4.5 ± 0.5 cm and 6.5 ± 0.5 cm respectively.
- The machine starts after pressing the <Start> button from behind a Start Line normal to the row of poles located between 25 and 35 cm from the centerline of the first pole. The minimum distance between the centerlines of two adjacent poles is 20 cm. Note that subsequently all distances with reference to the poles are measured from the centerline of the pole.
- The machine can hold a maximum of fifteen tires. It must autonomously detect the poles and stack tires depending on the following conditions:
    - The first pole must have two tires after the deployment operation
    - If a pole is within 30 cm of a previous pole, the total number of tires on this pole must be one. If not, it must be two.
- The operation terminates when either the machine runs out of tires and/or reaches the last pole or reaches the end of deployment range which is no more than 400 cm from the Start Line. The entire operation should not take more than three minutes. A LCD screen must display a termination message and communicate the following information as per the request of the user - operation time, number of tires deployed on each pole, number of tires on each pole after operation, total number of supplied tires, and number of poles and distance between their centerline and Start Line. [1]

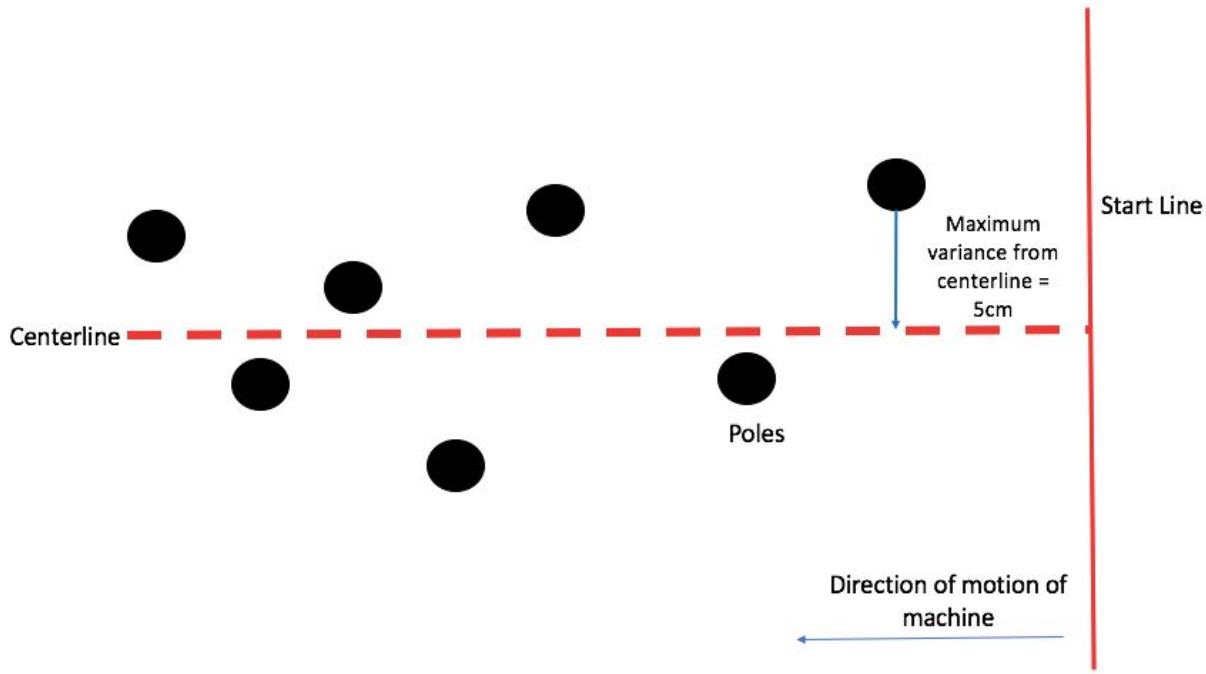

Figure 3.1.1: DIagram of Set Up described above

Our team strives to develop a functioning model that at least qualifies for the competition held by the client. Currently, this is our main focus. We would like to achieve more but will be realistic in our goal and work on improving upon it after we meet the minimum functionality.

3.2 OBJECTIVES

The team's goal is to develop a tire-deploying machine based on the following objectives. The objectives are listed in order of importance:

a. Accurate Functionality
    i. The machine can detect poles at their locations and the number of tires on the poles
    ii. The machine can accurately measure the correct distance from the Start Line to the first pole and distance between the poles
    iii. The machine can accurately measure the time taken to conduct the entire operation
b. Precise Movement
    i. The machine can precisely stop at the centerline of the base to deploy tires
    ii. The machine can deploy the correct number of tires exactly on the poles (where 'exactly' refers to the tires landing horizontally down the poles)
c. Manufacturability
    i. The design solution can be easily prototyped, given limitations in machining skill and less than 13 weeks to build it
    ii. The number of components (moving and fixed) is minimized

d. Reliability
    i. The machine can move a tire from its loaded position to the poles as per intended mechanisms
e. Efficiency
    i. The time taken to complete desired operation[1] is minimized
    ii. Power consumption of machine is minimized
f. Cost
    i. There is a minimal material cost involved in prototyping the solution
g. Compactness and Portability
    i. The design solution is of minimal volume and mass
h. Safety
    i. The machine stops when the emergency stop button is pressed
i. Usability
    i. The user can load tires onto the machine without much difficulty
    ii. The user can obtain desired information about operation on display with ease

3.3 METRICS

Metrics to measure a design's performance against objectives a-i are outlined below along with their units and utility graphs. They will later be used during decision making to evaluate and decide between alternatives.

a. Reliability (Accurate measurement)
    i. Number of successful detection of poles for every 10 poles. Successful detection includes both sensing the pole's presence and signalling that a pole has been detected
    ii. Difference between measured and actual distances, in cm

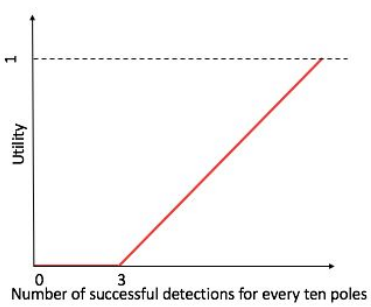

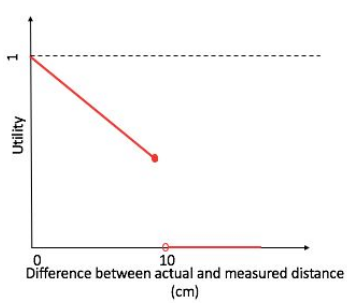

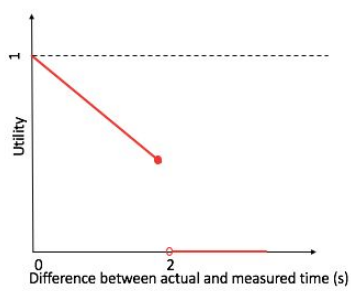

    iii. Difference between measured and actual times, in seconds
b. Precise Movement
    i. Distance between the centerlines of the base of the pole to that of the tire dispenser, in cm[2]
    ii. Number of tires left on poles after machine deploys them

[1] Desired operation refers to the operation the team specifies the machine should conduct, not the completion of the setup created by the client
[2] Assuming that tires will drop properly the closer the deployment mechanism is to the pole.

1. Two for the first pole
2. If distance between adjacent poles is less than 30 cm, then one tire, otherwise two tires

iii. Number of horizontally stacked tires for every 10 tires deployed

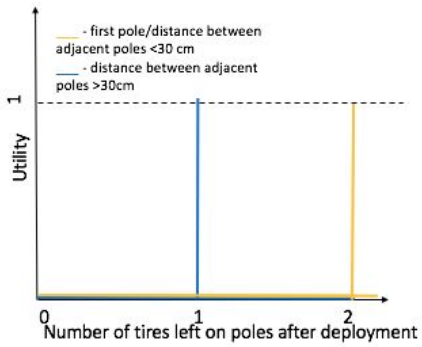

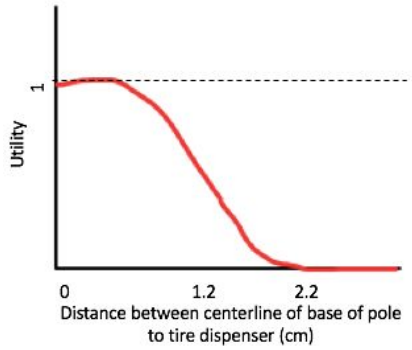

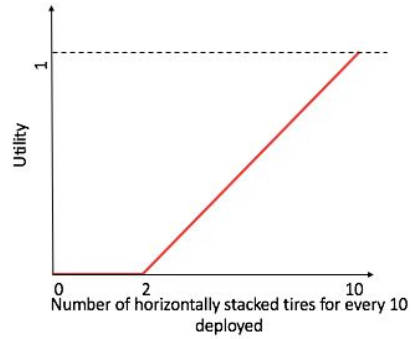

c. Manufacturability:
   i. Availability of materials, measured by the time taken for the material to be purchased to the time it can be received
   ii. Number of actuators and sensors needed

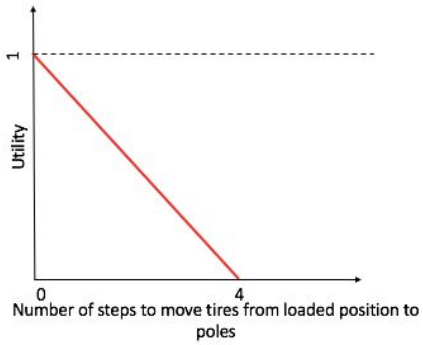

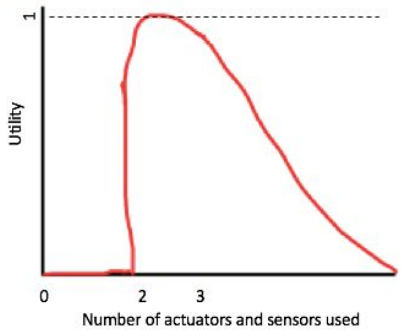

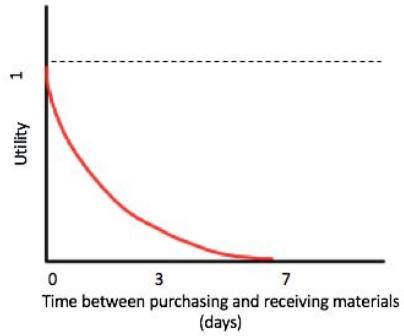

   iii. Number of steps taken by machine to deploy tires on poles from loaded position

d. Reliability:
   i. The number of times machine glitches in ten runs of the operation (where glitch refers to deviation from standard operation)

ii. The number of times the machine completely breaks down in ten runs of the

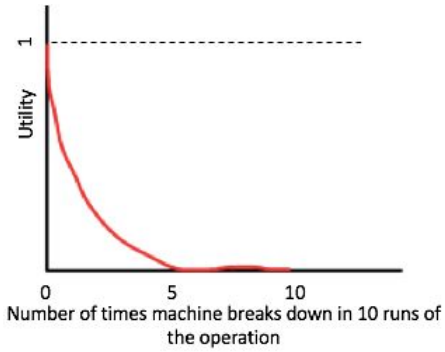

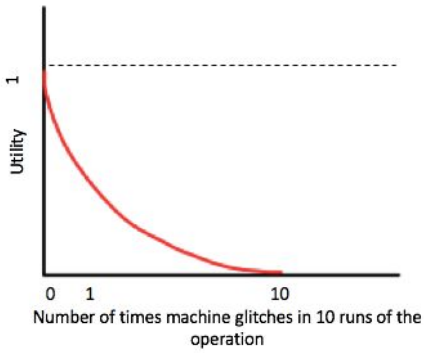

operation

e. Efficiency:
   i. The time taken for desired operation, in seconds

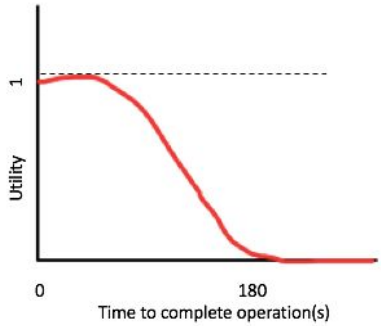

   ii. Power consumption of the robot for entire operation, in Watts[3]

f. Cost:
   i. The cost of the machine is determined by summing the cost of different components[4] (CAD)
      1. Market price of sensors, actuators, wheels and anything bought off shelf
      2. If any component is manufactured using 3-D printer, laser cutter, or CNC machine, cost will be $5 CAD per hour taken to manufacture

[3] Difficult to create utility function without knowing power requirements for the alternatives that will later be compared

[4] For parts purchased in foreign funds, exchange rate at the end of the business day of January 7th will be considered.

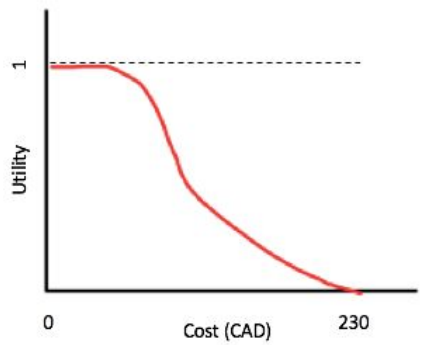

g. Compactness and Portability:
   i. The maximum volume of the machine accounting for any extension of parts, in cm^3
   ii. The mass of the machine, in kgs

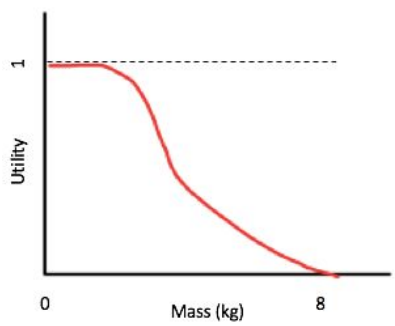

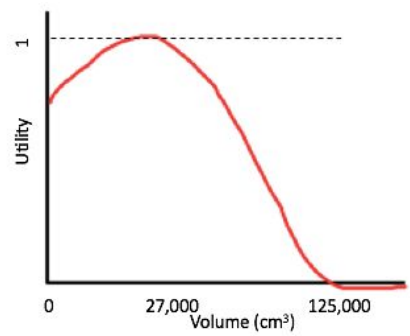

h. Usability:
   i. Time taken to load tires onto the machine and set up machine before operation, in minutes

i. TIme taken for user to obtain desired information about operation on display, in seconds

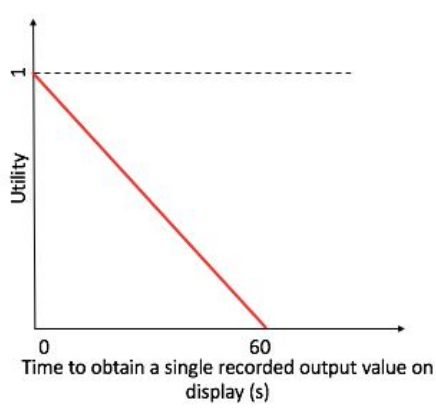

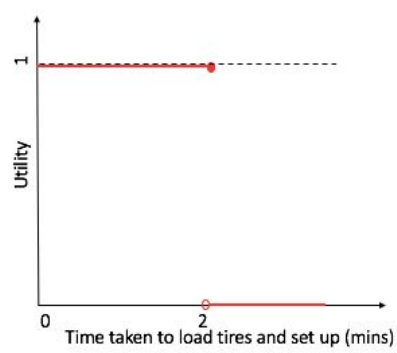

3.4 CONSTRAINTS

- The machine must be completely autonomous
- The machine must not present as a safety hazard to its user
- The prototype must fit within a $50 \times 50 \times 50\ cm^3$ envelope at all operation times and weigh no more than 8 kg
- The material cost must not exceed $230 (CAD) before shipping and taxes
- There must be an emergency stop switch that stops all mechanical moving parts immediately
- The machine must complete the desired operations and return to the Start Line after three minutes
- The time measured by the machine to conduct the operation must be within two seconds of the time measured by the referee
- The distances measured by the machine must be within 10 cm of the actual distances

3.5 FUNCTIONAL ANALYSIS

Glass Box Method [1]

This method is used to identify the overall functional requirements of a design by first only considering the inputs and outputs and asking questions about the steps for the transition from former to latter. This “black” box, then becomes “transparent” and specific functions are identified. The following is a broad outline of the functionality of the prototype being designed:

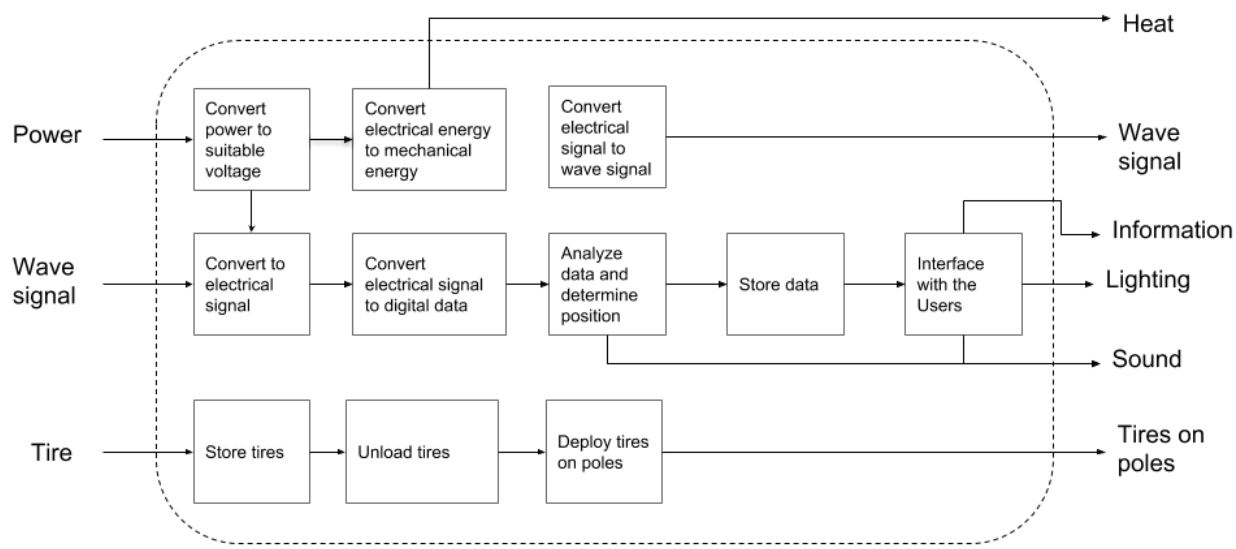

3.6 SURVEY

3.6.1 Literature Survey

Tire stacking is the process of storing tires efficiently either by placing horizontally oriented tires one on top of the other or vertically oriented tires side by side. According to Smithers Rapra's report titled *The Future of Tire Manufacturing to 2022*, global tire manufacturing output has been growing by 4% since 2016 and this trend is expected to continue till 2022 [2]. Further, the demand for tires is also expected to rise by 4% this year [3]. This increase in production and demand necessitates developments in automation [4].

Several tire manufacturing and distributing companies like Goodyear, Michelin, Canadian Tire, etc. are researching and developing solutions for automated storage and distribution. This is allowing them to improve customer service during peak seasons, increased warehouse and order fulfillment capacity for future growth and allows them to invest resources in continued development [5].

Another observation made based on the research done on existing solutions for tire stacking and storage is that they mostly involve storing vertically oriented tires horizontally. Studies have shown that vertical storage increases efficiency [B5] and thus further need is presented for the prototype being designed.

3.6.2 Idea Survey

AER201 Tire Stacking Machine (2011, Champion)

[6]

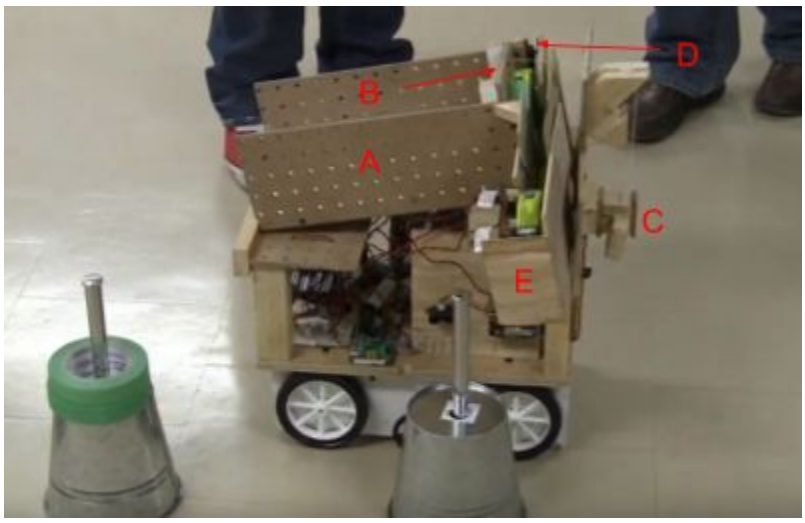

Figure 3.6.2.1. A photo of the Tire Stacking Machine prototyped by the champions of the 2011 AER201 competition.

Pictured above is a Tire Stacking Machine designed by an AER201 student team from 2011. Tires are stacked and horizontally loaded onto an incline (A). A wooden base (B) supports the stack from the bottom and advances the stack forward, driven by a motor and pulley (C). Once the stack advances and the machine detects a pole, a block of wood (D) kicks a tire down a narrow slide (E) and onto the pole.

While the above solution reliably loads masking tape onto poles that are aligned, it is not a suitable solution to the task of loading lightweight, rubber tires onto misaligned poles. First, the method of advancing the stack via sliding requires minimal friction between the tire and incline; but the tire, made of rubber, suffers high frictional forces and resists sliding motion. The narrow slide (E), with its walls, will likely cause high resistance due to friction as well. Second, the light weight of the rubber tires render the kicking motion (D) unreliable, as it may cause the tire to bounce due to the sudden impulse. Third, the machine is not well suited for stacking tires on poles that are misaligned, as it does not have a mechanism to extend and contract the slide based on the location of the pole.

AER201 Project (2011, Team 56)

[7]

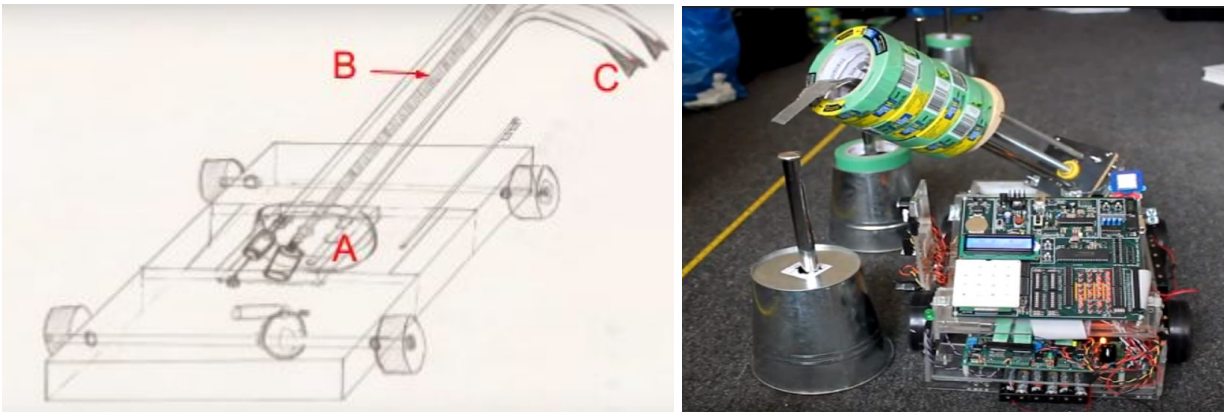

Figure 3.6.2.2. A schematic diagram (left) and photo (right) of the prototype for a tire stacking machine by Team 56 in 2011.

Above is a prototype designed by another AER201 group in 2011. Tires are stacked onto a wooden base (A) that is secured onto a linear rail shaft (B). As a motor rotates the shaft, the base advances and pushes the stack of tires upwards. Eventually, the tire at the top of the stack falls onto the pole, guided by a hook-like structure (C).

This prototype influenced the design of our proposed design. The use of a hook paired with a linear rail shaft can reliably deliver tires onto poles by guiding its movement. Furthermore, the use of the shaft and hook as both a way to store tires and to deploy them reduces the number of actuators in the machine, thereby decreasing material cost. Friction may not be of significant

concern with this design, as the shaft and advancing base provides enough control to the movement of the tires, unlike the aforementioned design which relies on the tire's rolling and sliding motions which can be easily affected by frictional forces.

US3955491A - Automotive Tire Stacking and Strapping Machine

[8]
This patent mentions the process of "down-stacking" wherein tire stacks are created by dispensing tires at a fixed level and subsequently lowering the created stack to add another tire at the same level. This idea was utilised while generating alternatives for methods of storing and dispensing tires.

A major disadvantage with this overall patent is that it creates stacks of a predetermined number of tires and does not allow flexibility in the number of tires being dispensed. It thus does not meet our requirement of dispensing tires based on certain criteria as mentioned in the problem formulation.

3.6.3 Market Survey

[9]
Storing tires on a tread is a common practice for facilities that need to store small quantities and large varieties. Potential customers include tire warehouse, and car dealers.

US6527499B2: Automated tire loading/unloading and compression system

[10]
This system is used for compactly storing a large number of tires into a tire transport frame. In order to compactly store the tires, a herringbone pattern is utilized as pictured on the right of Figure 3.6.2.1. The main use of this system is in large warehouses where tires are stored in frames for long-term storage [10] or for transportation purposes. The configuration of the stacked tires makes the system unsuitable for stacking tires onto poles. Furthermore, the system lacks mobility, which is needed for detecting the presence of randomly oriented poles on the ground.

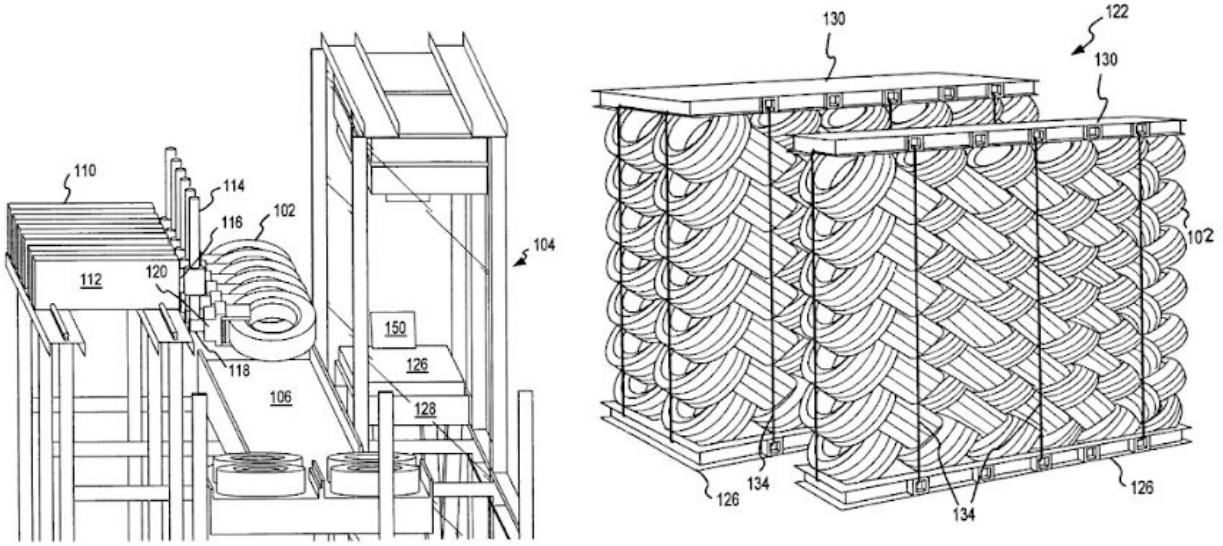

Figure 3.6.3.1. The automated tire loading/unloading system (left) and tires stacked in a herringbone pattern into a tire transport frame (right) [Y6]

US5562392A: Tire-stacking device and accessories for use in cooperative arrangement with a lift truck

[11]
This patent describes multiple accessories for use in cooperative arrangement with a lift truck, one of which is the coupling of a lift fork. Figure 3.6.3.2 shows the design overview of the arrangement. Tires are carried in a vertical stack on top of the fork lift, which is able to deploy tires in this vertically stacked configuration.

A scaled-down, dimensionally modified, and simplified version of the device can potentially serve as a viable solution to the problem addressed by this proposal. In particular, the fork-lift structure may serve as a more reliable mechanism by which to deploy tires on a pole, as an alternative to simply dropping the tires. A similar mechanism to this is considered as part of the alternative solutions discussed later in this proposal.

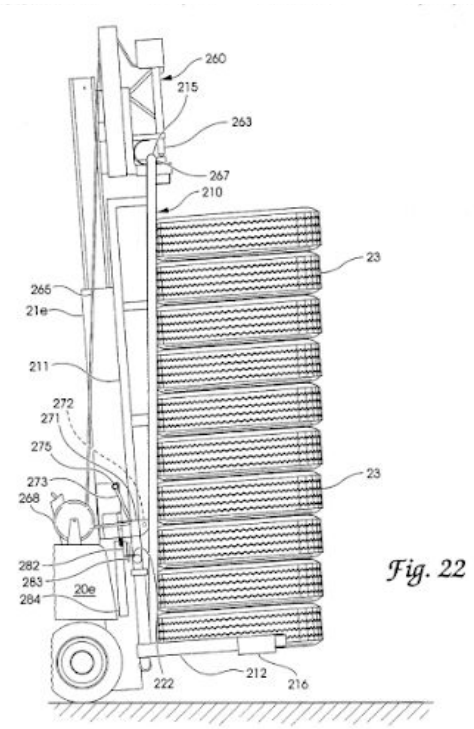

Figure 3.6.3.2. An accessory for use in cooperative arrangement with a lift truck (US5562392A) [11]

Conclusions from Survey:
On conducting background survey research, it has been found that automation in tire stacking and storage is a growing field because of increased demand and production. Several solutions exist and are being developed but they are large, costly and only stack a predetermined number of tires. Thus a need exists for an autonomous mobile platform to stack a varying number of tires based on detecting certain conditions.

The market and idea survey provided ideas that could be incorporated within the prototype being designed but also helped reject unfeasible or inadequate ones. The design solution would be light, low cost, autonomous, mobile and programmable to fit certain needs.

4 CONCEPTUALISATION

4.1 SUBMODULE BREAKDOWN

The overall design can be broken down to several submodules, which each fulfill a function. Some submodules are required to move in one direction, which can be seen in Figure 4.1.1. Submodules are listed below:

1. Stacking/unstacking: allow the user to stack multiple tires and automatically unstack 1 to 2 each time

2. Deployment: Place 1 to 2 tires onto a pole each time
3. Extension: Extent at least 10 cm in left and right direction
4. Detection: detect the position of poles(bases) in left and right direction and the number of tires
5. Indication: indicate the successful detection and deployment
6. Microcontroller: control the system

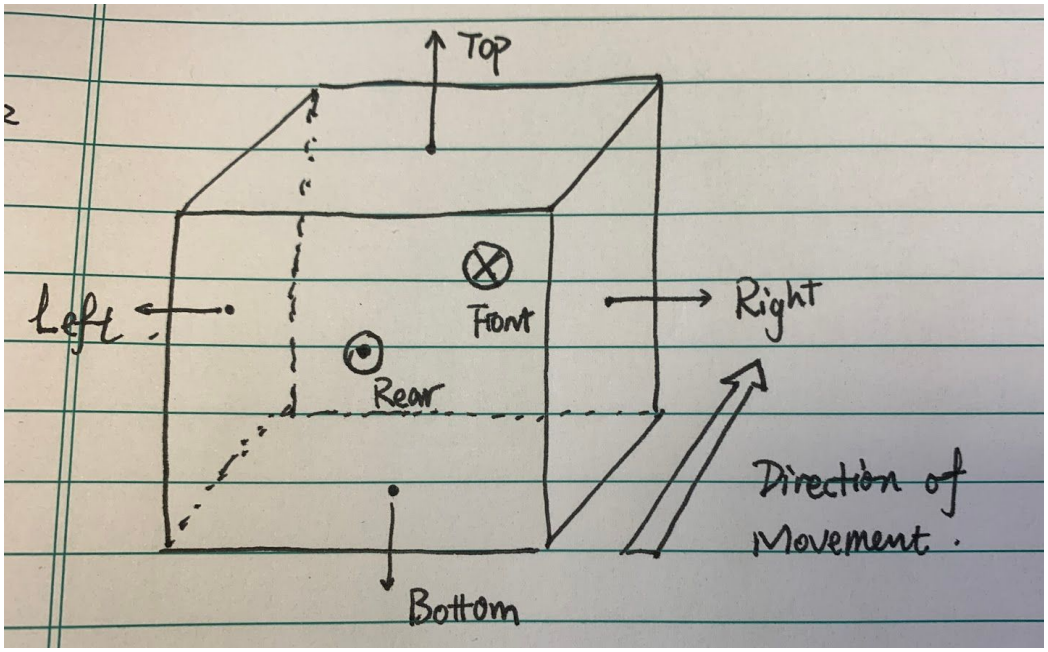

Figure 4.1.1. Relative directions of the machine and its movement.

4.1.1 Path of movement

As described in the problem deformation, poles are located along an imaginary line with a variance of 5 cm. The path of the machine restricts its maximum volume and the structure of its framework. This factor also determines functional decomposition and submodule analysis. There are two possible routines along which a machine can visit all poles: one is travelling over all poles and the other is moving by the side of poles (Figure 4.1.1.1). The team decided on moving by side of the pole earlier in the decision making process. Because many detailed design is different in these two scenarios. This decision did not limit the design space but benefited the team to generate more reliable ideas.

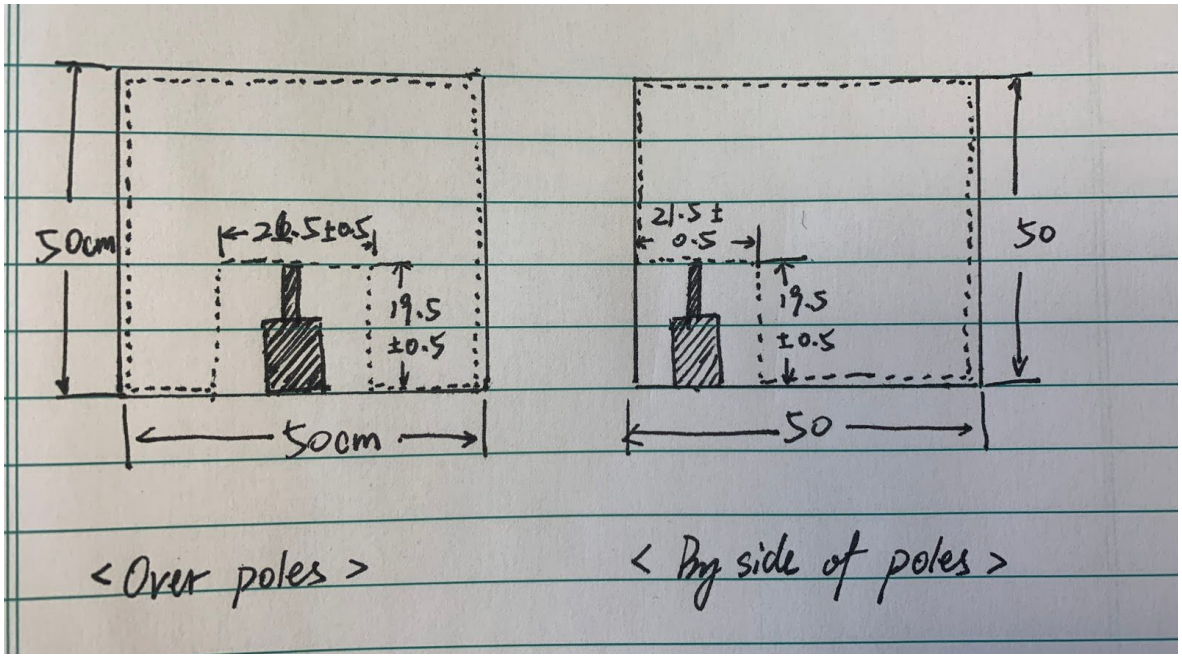

Figure 4.1.1.1. Different volume constraints depending on the path of movement

4.2 ALTERNATIVE SOLUTIONS

4.2.1 Submodule 1: Stacking and unstacking mechanism

1. **Tube and hook system**

Tires are hung horizontally onto a pipe with hook at the end. To load the tires, the user threads them from the hooked end until it touches a platform at the other end. The platform is driven by a motor and pushes a desired number of tires out from the angled end. This system transforms circular movement of the motor to linear movement of the platform. It also fulfills the functionality of deploying tires onto poles (Submodule 2).

<u>Pros:</u> High precise movement; Simple manufacturability.

<u>Cons:</u> Medium compactness; High cost.

Figure 4.2.1.1 The sketch (left) and prototype (right) of the tube and hook system

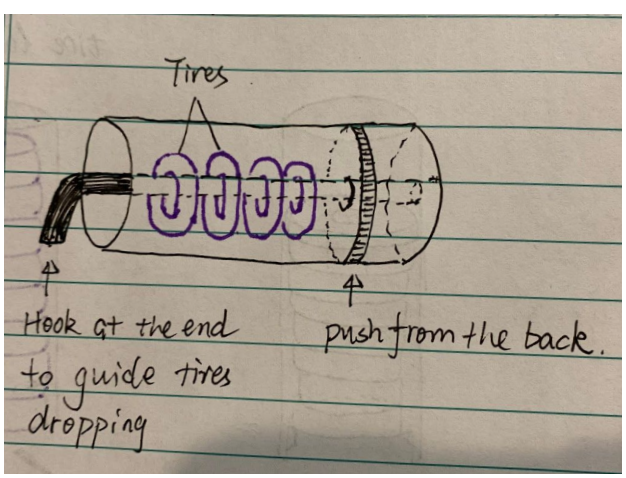

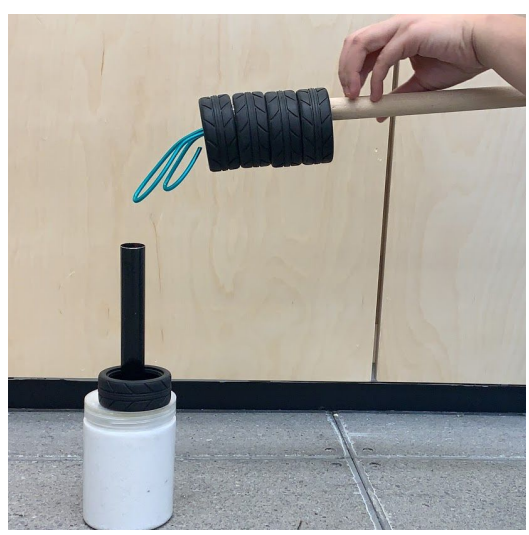

2. Pulley-weight system

This is a passive stacking system. Tires are vertically stacked and unstacked from the top. Tires are pushed up by the base from the bottom due to the gravity of external weights. External weights are hung across a pulley and attached to the base. There are three slots on the side of the other tube through which the weights are hung, so that the base can move freely while being guided by the slots. Figure 4.2.1.2 shows the system break down and a preliminary prototype.
<u>Pros:</u> High compactness (can be placed below the deployment system); Low cost.
<u>Cons:</u> Poor manufacturability; Poor reliability (See 4.3.1. Testing)

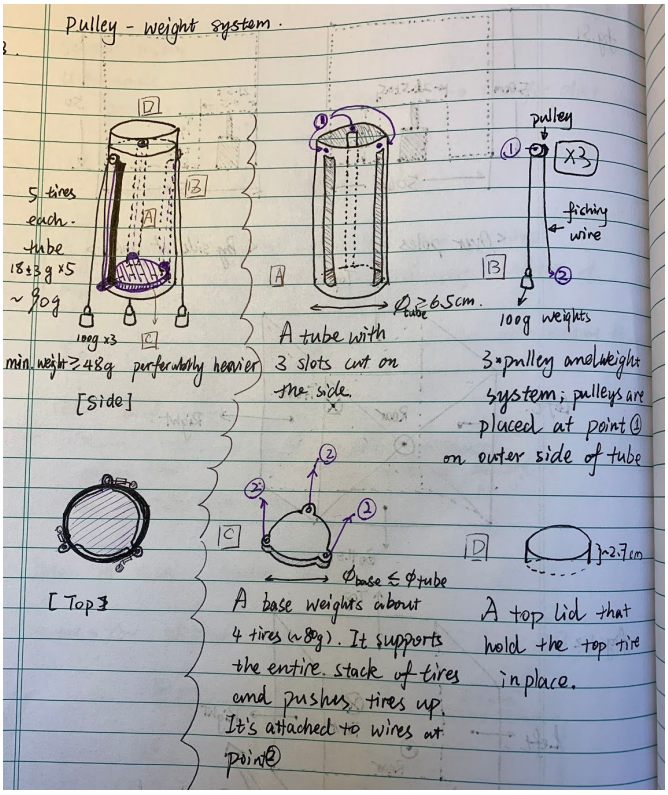

Figure 4.2.1.2 Sketch, description (left), and prototype (right) of the pulley-weight system. In the prototype, bags of salts represent the external weights.

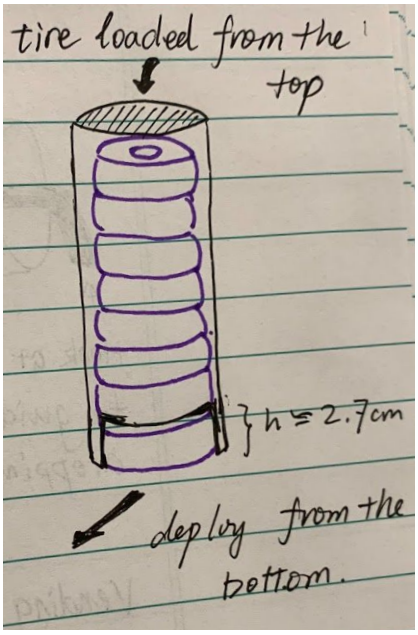

Figure 4.2.1.3 Sketch of the self-weight system

3. Self-weight system

Comparing to the pulley-weight system, the directions of unstacking in the self-weight system are reversed, i.e. from the bottom. The space left for deploying is about the height of a tire ~2.7 cm. The system is driven by the self-weight of tires.

<u>Pros:</u> Simple manufacturability; Low cost; High usability;
<u>Cons:</u> Poor compactness (close to height limit);

4. Vending machine mechanism

This system consist of two parts: the outer frame and the spring coil. The outer frame is wooden and covered by a sheet of styrene at the top. Styrene sheet is bent into a U shape holding the tires, which are stacked vertically between the coils. The spring coil is made from aluminum with a inner diameter slightly larger than that of the tires and a outer diameter smaller than that of the tires. The spring coil can be driven by a DC motor.

Pros: Medium compressibility; High precise movement
Cons: Complex manufacturability; Poor reliability (See 4.3.1)

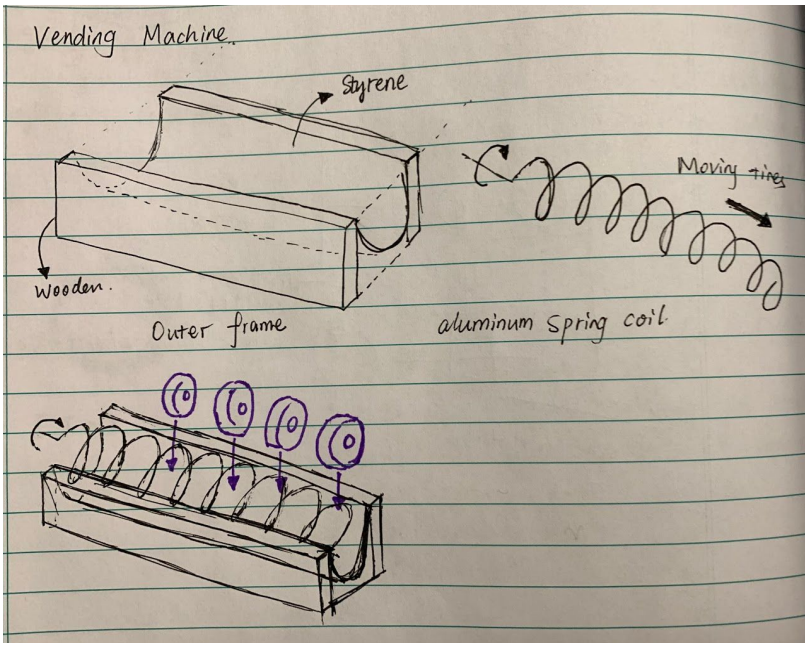

Figure 4.2.1.4 Sketch (left) and prototype (right) of the vending machine system.

4.2.2 Submodule 2: Deployment mechanism

1. **Tube and hook system See 4.2.1 for details.**
2. **Conveyor belt system**

This system is another way to convert rotating motion into a linear motion using timing belts. A thick rubber band is wrapped around two shafts and the shafts are connected by a timing belt to keep the rotation of both shafts at the same angular velocity. To deploy a tire on top of it, the conveyor belt is driven by a motor and proves horizontal velocity. The tire is accelerated, bounced from a platform underneath the belt and then deployed onto the pole.
Pros: High efficiency;
Cons: Medium precise movement; Complex manufactuability.

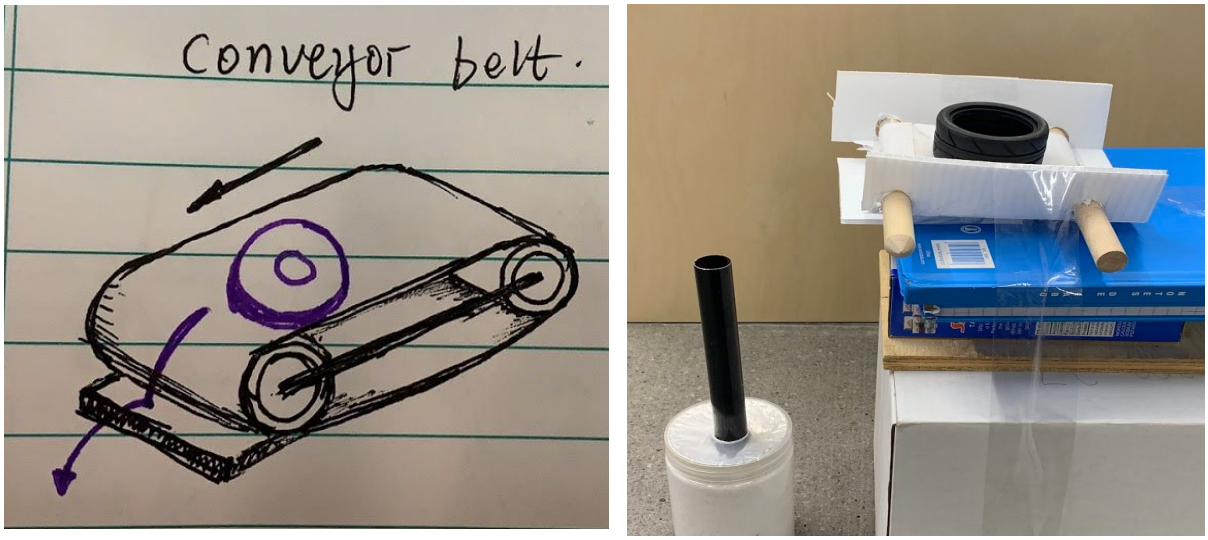

Figure 4.2.2.1 Sketch (left) and prototype (right) of the conveyor belt system

3. Trap door

The trap door system has two stage as can be seen in 4.2.2.2. As soon as the centerline of the trap door aligned with the centerline of the pole, motors are started and drop tires onto a pole.
Pros: High efficiency; Simple manufacturability;
Cons: Medium precise movement; Low reliability

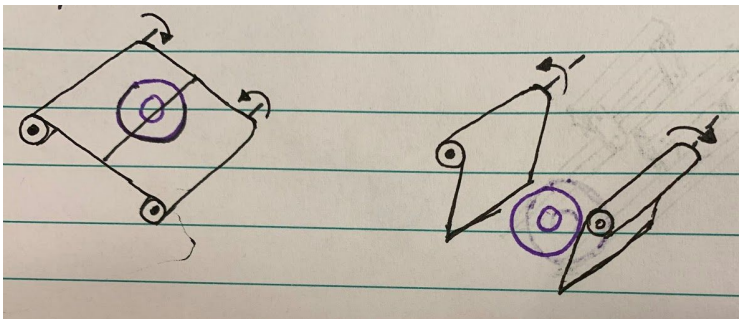

Figure 4.2.2.2 Sketch of two stages of trap doors

4. Forklift

As can be seen in Figure 4.2.2.3., the forklift system includes three states. It first locates above the pole, start decreases its height and place the tire onto the base of a pole, and then turn back to original position.
Prons: High precise movement; High reliability
Cons: Difficult to manufacture; High Cost; Slow movement

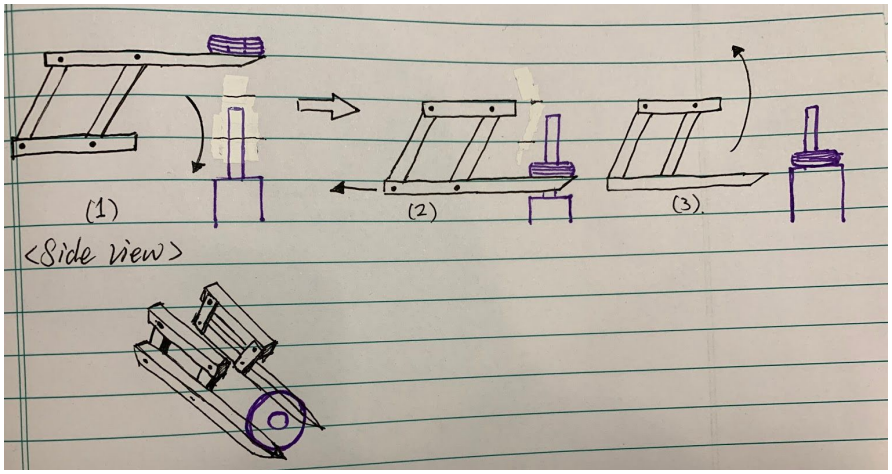

Figure 4.2.2.3 Sketch of forklift and how it place a single tire

4.2.3 Submodule 3: Extension mechanism

The following are common extension mechanism used in the industry [12]

1. Lead screw
2. Linear motion rail
3. Rack and pinion
4. Telescope+timing belt

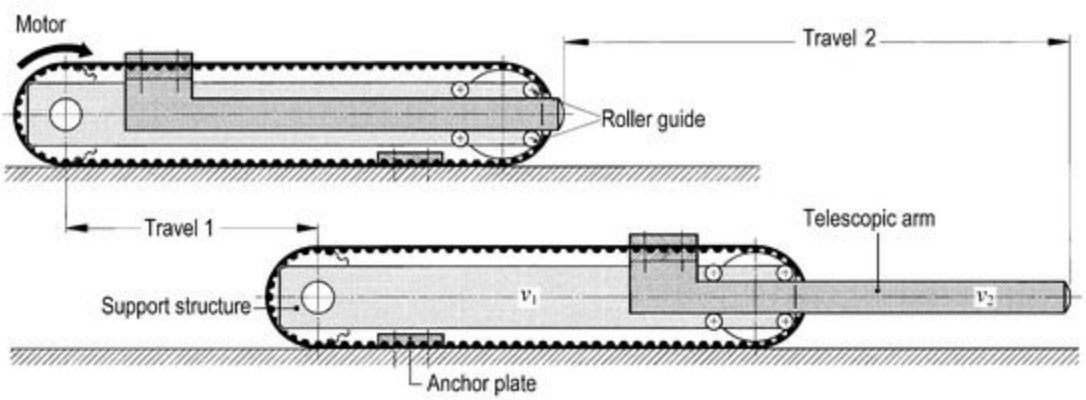

Figure 4.2.3.1 A telescopic extension mechanism driven by timing belt [13]

4.2.4 Submodule 4: Sensors

Due to the moving path and requirement of accuracy, choice of sensors are limited. IR and ultrasonic sensors are able

1. Ultrasonic sensor HC-SR04 (range 2cm - 400cm) [14]
   Pros: High reliability; Medium cost;
   Cons: Medium accurate measurement
2. IR proximity sensor gp2y0a41sk0f (range 4cm - 30cm) [15]
   Pros: High reliability; High accurate measurement
   Cons: High cost; Analog input

3. IR obstacle avoidance sensor B077GMFS1K (range 2cm - 30cm; *Actual range is less than 10cm) [16]
   Pros: Low cost;
   Cons: Low reliability; Poor accurate measurement;

4.2.5 Submodule : Microcontroller and development board

1. PIC18F4620 and AER201 development board
   Pros: High reliability;
   Cons: High cost;
2. Arduino boards, e.g.
   Pros: Modularized, simple manufacturability
   Cons: Medium debugging ability;
3. Custom board:
   Pros: Low cost;
   Cons: Medium debugging ability;

4.2.6 Alternative systematic designs

The team has considered other combinations of the submodules.

4.3 DECISION MAKING

Two decision-making techniques - utility based and analytical hierarchy process - were used to determine which alternatives from the ones above meet our aforementioned objectives. While tests were performed to collect data for some metrics, research and logical reasoning was used for others. [1]

4.3.1 Testing Protocol and Results

The team built few preliminary prototypes and conducted testing according to the protocol as follows.

Function: Stacking and Deployment Mechanism
Goal: Determine the design for proposal based on the result of testing prototypes. Mainly observation.
Prototype: (As explained in Section 4.2.1 and 4.2.2, images of prototypes are als)

1. Tube and hook
2. Pulley-weight
3. Self-weight
4. Vending machine
5. Conveyor belt
6. Forklift

Results: According to our observations, the tube and hook system deployed tires most accurately for more runs and also the storage of tires and maintenance of their position in the loaded state was more reliable.

Function: detecting poles and tires

Goal: determine the type and number of sensors based on their accuracy.

Base detection:

1. Place the base at different distances (10-20 cm, 2 cm apart). For each distance take 3 readings of values outputted by the sensor. Average the readings and check how accurate they are with respect to the actual measured distance.
2. Place different sensors along a line. Move the base along with another line that is parallel to the first one 5,10 or 15 cm away from it.

Tire detection:

1. Place two tires on a pole. Place different sensors at the same height as each tire each time. Repeat with different distance (5-15 cm, 2 cm apart)

Choices:

1. Ultrasonic sensor [HC-SR04] (range 2cm - 400cm)
2. Infrared proximity sensor [Sharp GP2Y0A41SK0F] (range 4cm - 30cm)
3. IR obstacle avoidance sensor [B077GMFS1K] (range 2cm - 30cm)

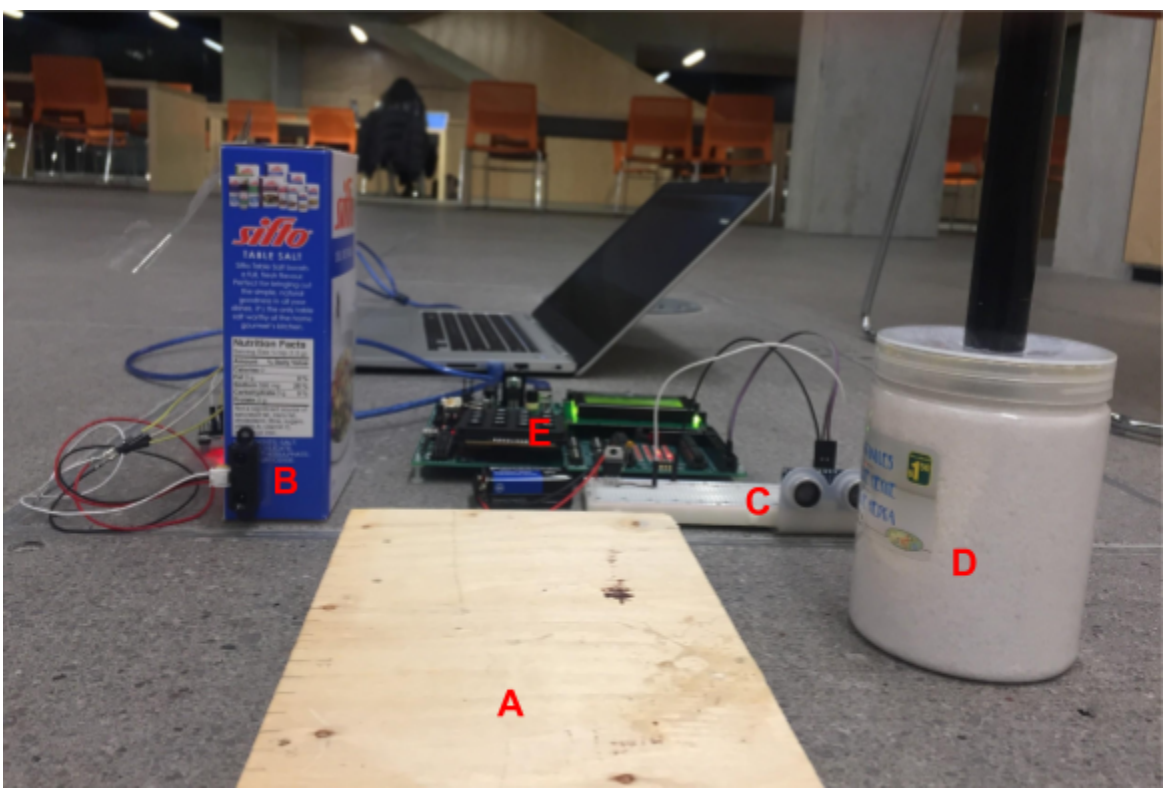

Figure 4.3.1.1: Apparatus for sensor test
(A: Distances marked on plank, B: IR sensor; C:Ultrasonic Sensor, D: Base, E: PIC Board)

Results: Refer to Appendix Section 2 for the numerical data obtained from the trials. The tests proved that the IR proximity sensor was much more accurate than either ultrasonic or IR obstacle avoidance.

4.3.2 Analytical Hierarchy Process

This section shows sample calculations for the Stacking and Unstacking Submodule. AHP for the other submodules is in Appendix Section 1. For AHP, the alternatives were first compared in pairs for a given objective and given a rating based on the following table as outlined in Professor Emami's lecture slides [17].

Judgement of Preference/Importance	Numerical Rating
Extremely (Preferred/Important)	9/8
Very Strongly (Preferred/Important)	7/6
Strongly (Preferred/Important)	5/4
Moderately (Preferred/Important)	3/2
Equally (Preferred/Important)	1

4.3.2.1 Relative Preference and Relative Importance Matrices

The RP matrices each pertaining to a single objective only were created for alternatives for different submodules mentioned above. The alternatives were compared pairwise, the matrices were normalised and then each alternative was given an overall preference. RI matrices depict the relative preference of the objectives with respect to each other. The same procedure as for RP matrices was also followed for RI.

RP Matrices for Stacking Mechanism

Precision RP Matrix					Normalized Precision RP Matrix					Overall Preference
	Tube & Hook	Pulley & Weight	Self-Weight	Vending		Tube & Hook	Pulley & Weight	Self-Weight	Vending	
Tube & Hook	1	7	3	9	Tube & Hook	0.63	0.519	0.682	0.529	0.589
Pulley & Weight	1/7	1	1/5	2	Pulley & Weight	0.09	0.074	0.045	0.118	0.082
Self-Weight	1/3	5	1	5	Self-Weight	0.21	0.37	0.227	0.294	0.275
Vending	1/9	1/2	1/5	1	Vending	0.07	0.037	0.045	0.059	0.053

Manufacturability RP Matrix					Normalized Manufacturability RP Matrix					Overall Preference
	Tube & Hook	Pulley & Weight	Self-Weight	Vending		Tube & Hook	Pulley & Weight	Self-Weight	Vending	
Tube & Hook	1	6	1/2	1	Tube & Hook	0.24	0.429	0.185	0.286	0.285
Pulley & Weight	1/6	1	1/5	1/2	Pulley & Weight	0.04	0.071	0.074	0.143	0.082
Self-Weight	2	5	1	1	Self-Weight	0.48	0.357	0.370	0.286	0.373
Vending	1	2	1	1	Vending	0.24	0.143	0.370	0.286	0.260

Reliability RP Matrix					Normalized Reliability RP Matrix					Overall Preference
	Tube & Hook	Pulley & Weight	Self-Weight	Vending		Tube & Hook	Pulley & Weight	Self-Weight	Vending	
Tube & Hook	1	7	3	9	Tube & Hook	0.63	0.677	0.632	0.529	0.617
Pulley & Weight	1/7	1	1/2	3	Pulley & Weight	0.09	0.097	0.105	0.176	0.117
Self-Weight	1/3	2	1	4	Self-Weight	0.21	0.194	0.211	0.235	0.212
Vending	1/9	1/3	1/4	1	Vending	0.07	0.032	0.053	0.059	0.053

Efficiency RP Matrix					Normalized Efficiency RP Matrix					Overall Preference
	Tube & Hook	Pulley & Weight	Self-Weight	Vending		Tube & Hook	Pulley & Weight	Self-Weight	Vending	
Tube & Hook	1	5	4	1/2	Tube & Hook	0.290	0.278	0.480	0.257	0.326
Pulley & Weight	1/5	1	1/3	1/9	Pulley & Weight	0.058	0.056	0.040	0.057	0.053
Self-Weight	1/4	3	1	1/3	Self-Weight	0.072	0.167	0.120	0.171	0.133
Vending	2	9	3	1	Vending	0.580	0.500	0.360	0.514	0.488

Cost RP Matrix					Normalized Cost RP Matrix					Overall Preference
	Tube & Hook	Pulley & Weight	Self-Weight	Vending		Tube & Hook	Pulley & Weight	Self-Weight	Vending	
Tube & Hook	1	1/5	1/2	1	Tube & Hook	0.111	0.124	0.088	0.077	0.100
Pulley & Weight	5	1	4	6	Pulley & Weight	0.556	0.619	0.702	0.462	0.584
Self-Weight	2	1/4	1	5	Self-Weight	0.222	0.155	0.175	0.385	0.234
Vending	1	1/6	1/5	1	Vending	0.111	0.103	0.035	0.077	0.082

Compactness RP Matrix					Normalized Compactness RP Matrix					Overall Preference
	Tube & Hook	Pulley & Weight	Self-Weight	Vending		Tube & Hook	Pulley & Weight	Self-Weight	Vending	
Tube & Hook	1	1/3	6	1	Tube & Hook	0.194	0.186	0.286	0.194	0.215
Pulley & Weight	3	1	8	3	Pulley & Weight	0.581	0.558	0.381	0.581	0.525
Self-Weight	1/6	1/8	1	1/6	Self-Weight	0.032	0.070	0.048	0.032	0.045
Vending	1	1/3	6	1	Vending	0.194	0.186	0.286	0.194	0.215

Usability RP Matrix					Normalized Usability RP Matrix					Overall Preference
	Tube & Hook	Pulley & Weight	Self-Weight	Vending		Tube & Hook	Pulley & Weight	Self-Weight	Vending	
Tube & Hook	1	3	1/5	1	Tube & Hook	0.136	0.214	0.130	0.136	0.154
Pulley & Weight	1/3	1	1/7	1/3	Pulley & Weight	0.045	0.071	0.093	0.045	0.064
Self-Weight	5	7	1	5	Self-Weight	0.682	0.500	0.648	0.682	0.628
Vending	1	3	1/5	1	Vending	0.136	0.214	0.130	0.136	0.154

Objective RI Matrix							
	Precision	Manufacturability	Reliability	Efficiency	Cost	Compactability	Usability
Precision	1	2	3	4	5	5	9
Manufacturability	0.5	1	2	3	4	4	8
Reliability	0.333	0.5	1	2	3	3	7
Efficiency	0.25	0.333	0.5	1	2	2	6
Cost	0.2	0.25	0.333	0.5	1	1	5
Compactability	0.2	0.25	0.333	0.5	1	1	5
Usability	0.111	0.143	0.143	0.167	0.2	0.2	1

Normalized Objective RI Matrix								Overall Preference
	Precision	Manufacturability	Reliability	Efficiency	Cost	Compactability	Usability	
Precision	0.386	0.447	0.41	0.358	0.309	0.309	0.22	0.348
Manufacturability	0.193	0.223	0.274	0.269	0.247	0.247	0.195	0.235
Reliability	0.128	0.112	0.137	0.179	0.185	0.185	0.171	0.157
Efficiency	0.096	0.074	0.068	0.09	0.123	0.123	0.146	0.103
Cost	0.077	0.056	0.046	0.045	0.062	0.062	0.122	0.067
Compactability	0.077	0.056	0.046	0.045	0.062	0.062	0.122	0.067
Usability	0.043	0.032	0.02	0.015	0.012	0.012	0.024	0.023

Consistency Check

The RP and RI Matrices were then checked for consistency by calculating the CI values and ensuring they are less than 0.1.

Matrix	Consistency Index	Consistency Ratio
Precision	0.032	0.006
Manufacturability	0.069	0.013
Reliability	0.02	0.004
Efficiency	0.037	0.007
Cost	0.054	0.01
Compactability	0.028	0.005
Usability	0.025	0.005
Objectives	-0.216	-0.048

Clearly all the CI values are much less than 0.1 and hence the matrices are consistent.

Final Decision

The total preference was then calculated by multiplying the overall preference for the alternative for a specific objective with that for the objective being used and the one with the highest was chosen for the proposed machine.

Total Preference	
Tube & Hook	**0.446**
Pulley & Weight	0.131
Self-Weight	0.270
Vending	0.153
Tube & Hook wins!	

The ‘Tube and Hook’ alternative has by far a greater total preference than the other alternatives and was thus chosen in the proposed design as discussed later.

4.3.3 Utility Based Decision Making

This decision making tool was used for the Deployment Submodule because total preference values for and were very close to each other (refer to Appendix Section 1). This was done in the hopes that the decision would be made even clearer.

Utility Based Decision Making										
			Tube and Hook		Conveyor Belt		Trap Door		Fork-lift	
Objectives	Weight	Metric	Estimated Value	Utility Value	Estimated Value	Utility Value	Estimated Value	Utility Value	Estimated Value	Utility Value
Precise Movement	4	Number of horizontally stacked tires for every 10 tires deployed	10	1	3	0.125	3	0.125	4	0.25
Manufacturability	3	Number of actuators needed[5]	5	0.7	6	0.6	4	0.8	4	0.8
		Number of steps taken by machine to deploy tires on poles from loaded position	1	0.75	3	0.25	2	0.5	2	0.5
Efficiency	2	The time taken for desired operation, in seconds[6]	12	0.7	30	0.1	10	0.75	25	0.2
Cost [7]	1	Cost of parts, in CAD	20	0.91	36	0.84	18	0.92	50	0.5
Utility Weighted Sum			10.66		4.09		6.82		5.8	
Normalised Total			0.39		0.15		0.25		0.21	

[5] Sensors not considered since deployment mechanism is not dependent on detecting poles
[6] Maximum value in utility graph changes to 35s since we are only considering deployment operation time
[7]Maximum value in utility graph changes to $100 since we are only considering cost of submodule

Performing utility based decision making has thus been very useful since it is clear now that Tube and Hook is the preferred option.

4.4 SPECIFICATION

This section describes and analyses the selected solution. It is divided into three parts: electromechanical design, circuit design, and microcontroller design.

4.4.1 Electromechanical Design

This section outlines the design solution from the electromechanical perspective. It discusses different components of the design solution and how they will be used to achieve certain functions. Diagrams with dimensions are included as well. Note that the dimensions are meant to be estimates, and may be subject to small changes.

Design Overview

The chosen design fits within an envelope of 37.1cm x 31.6cm x 31.3cm at all operation times and its geometry is shown in Figure 4.4.1.1. Everything is mounted on a main framework that has the dimensions of 27.1cm x 23.5cm x 31.3cm. On top of the frame, two tubes of square cross section are attached and have a hook-like rod structure hanging out towards the right side of the frame. They can each hold a maximum of 8 tires beaded through the rod structure. Tires are deployed onto the pole by sliding them down the hook. As indicated in the Figure, the tubes are able to slide side to side to position the hook directly over a detected pole.

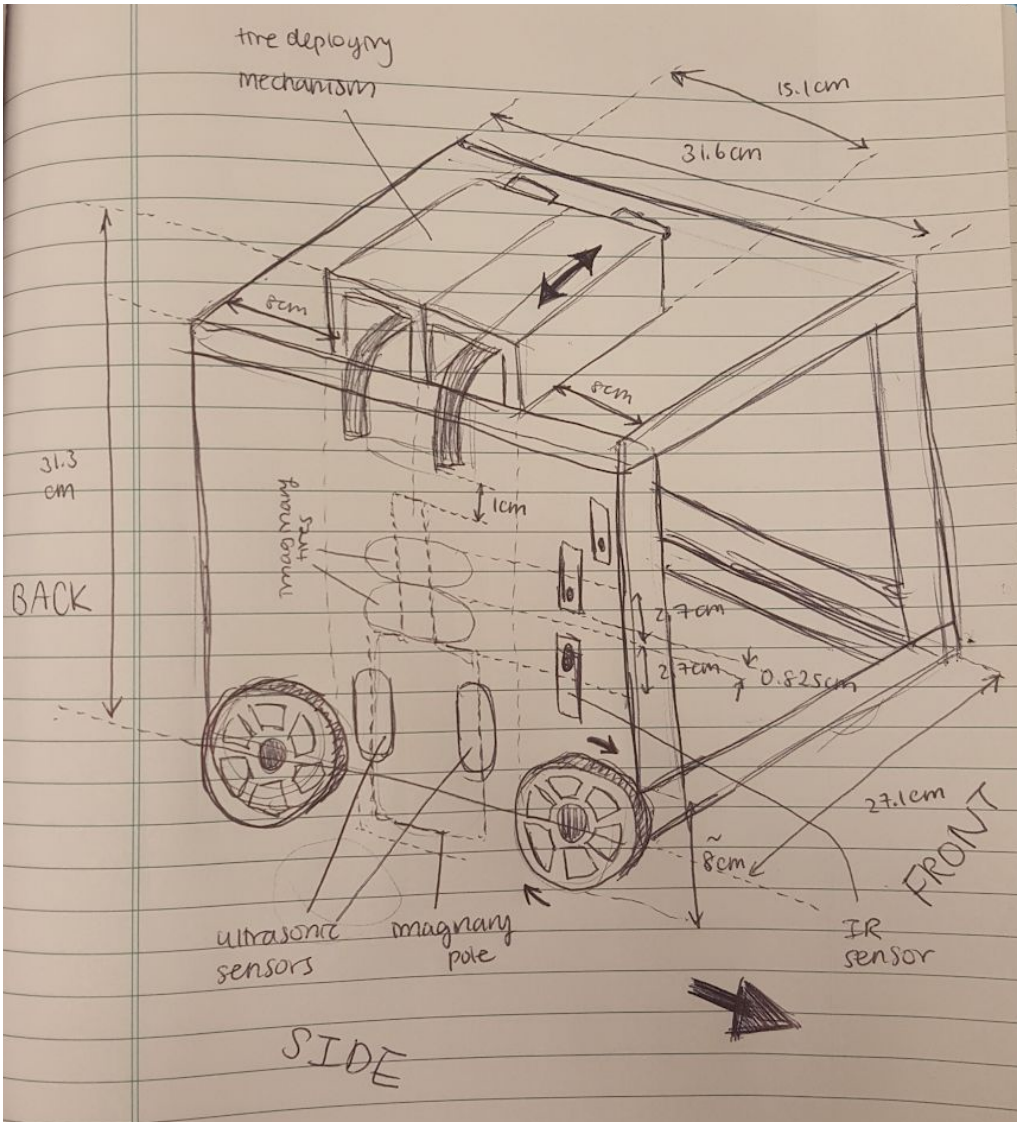

Figure 4.4.1.1. Diagram of the chosen design

The direction of the machine's movement is indicated in Figure 4.4.1.1. Because the tubes are able to slide to position the hooks precisely over the poles, no steering mechanism is needed; the machine will simply move forwards or backwards.

Tire Advancement and Deployment System

A sketch of the system of a hook (A) within a square tube (B) is shown in Figure 4.4.1.2. The system functions as the tire advancement and deployment system. Initially, the user stacks a set of tires into two sets of tubes as in Figure 4.4.1.2. Note that the tires must be stacked so that the hook (or rod) runs through the holes of the tires. Since there are two sets of tubes in total, each tube must hold either 7 or 8 tires to begin with. The end of the stack rests on a 5mm-thick wooden platform (C), which is attached to a lead screw (D) by screwing the nut (E) on the lead screw onto the platform. The lead screw is attached to a stepper motor (F), so that when the

motor spins, the platform advances forwards. In order to deploy one tire at a time, the stepper motor is controlled so that the wooden platform advances by the thickness of a single tire (2.7 cm) each time. The hook guides the direction and motion of the tire so that it is able to be deployed precisely on top of the poles.

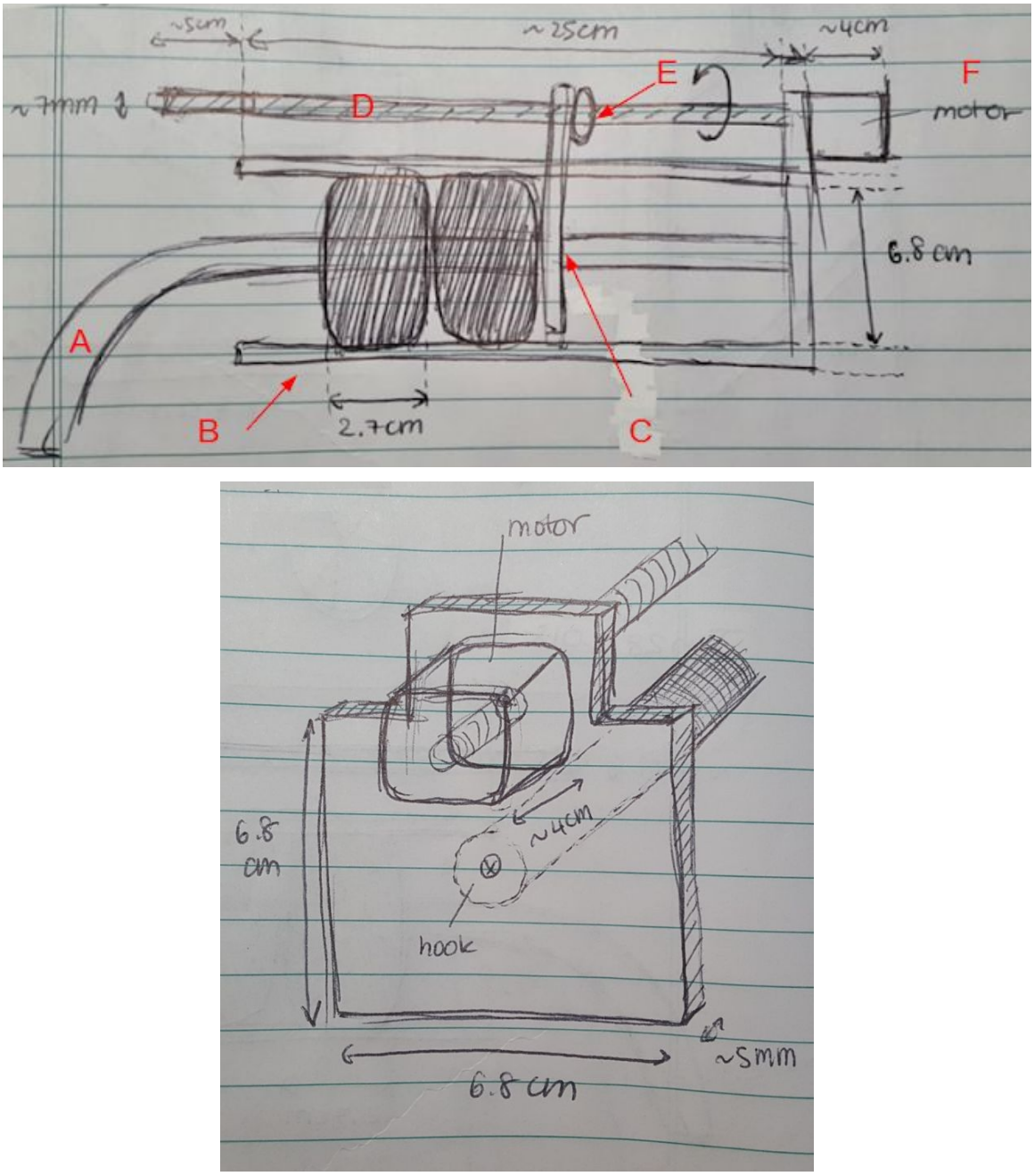

Figure 4.4.1.2. (Top) A side view of the tire advancement and deployment system. (Bottom) View of the tire advancement and deployment system from the motor end (i.e. the back view).

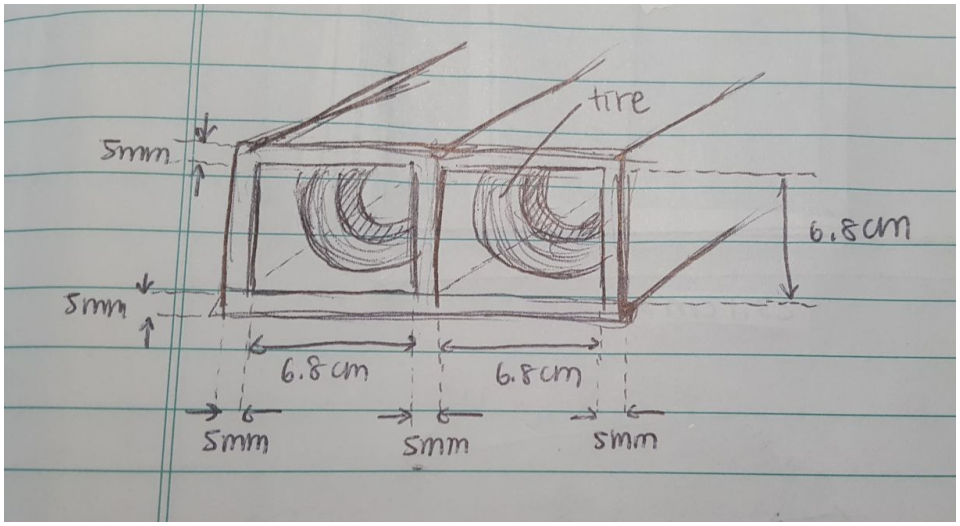

Figure 4.4.1.3. A front view, with dimensions, of the rectangular tubes with tires within them. The hook was not drawn for simplicity.

In order to ensure that the platform can be attached to the lead screw that is outside of the rectangular tube, it is required that the tube has a slit of approximately 2 cm in width running from a few cm away from the end of the tube to the opening of the tube, as seen in Figure 4.4.1.4. The length of this slit should be approximately 21.6 cm, which is equal to the length of 8 horizontally stacked tubes. This slit allows for the platform (see Figure 4.4.1.4 for its geometry) to extend beyond the tube and to be attached to the nut. As seen in Figure 4.4.1.4, the platform is a 6.5 cm x 6.5 cm square with a small extension at the top that would slide along the slit.

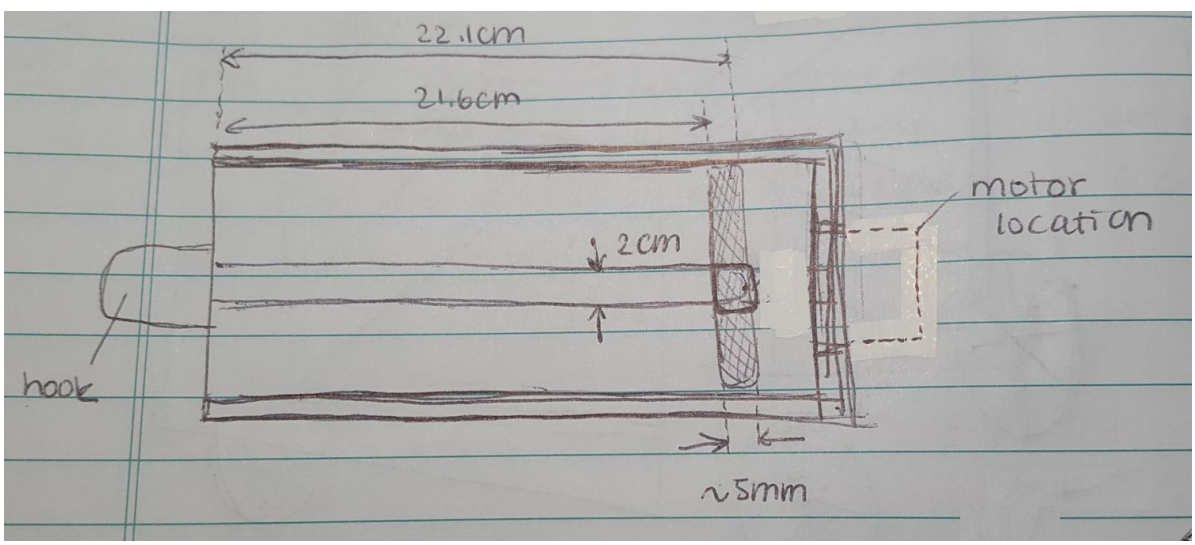

Figure 4.4.1.4. A top view of the square tube. A slit of 2 cm-width runs along its length up to the opening of the tube on the left.

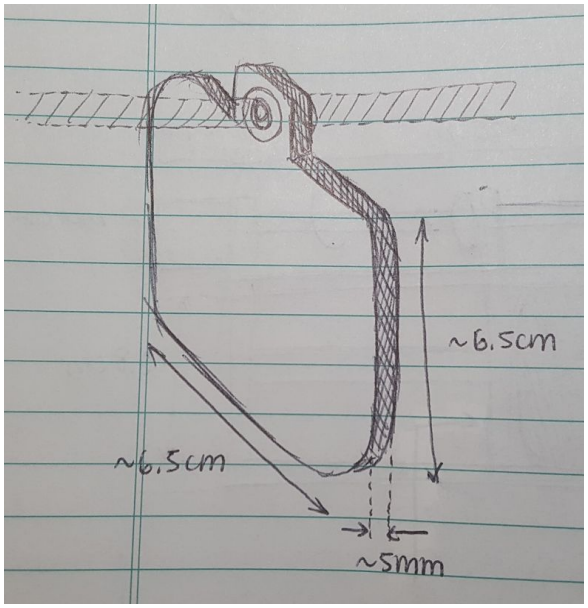

Figure 4.4.1.5. Diagram and dimensions of the wooden platform. The extension on top of the platform will allow the platform to move along the lead screw as pictured.

Extension System

Unlike the tire advancement and deployment system which simply pushes a tire down the hook, the extension system positions the hook so that the tire can be deployed precisely on top of the detected pole. It does this by providing a mechanism by which the two tubes of square cross-section extend and contract, away from and towards the body of the machine, respectively.

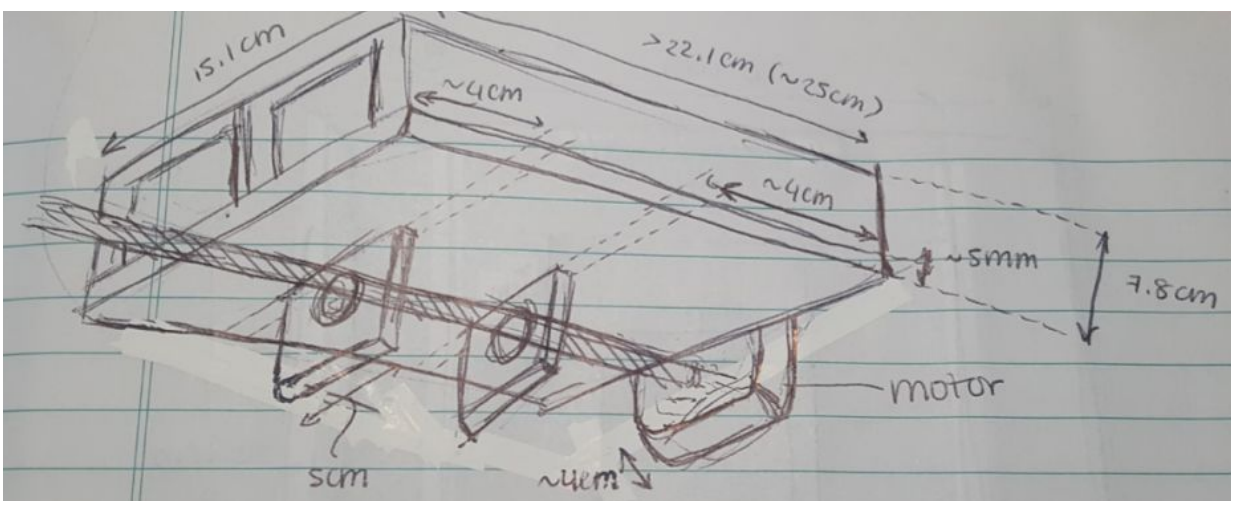

Figure 4.4.1.6. Bottom view of the two tubes.

The extension and contraction are achieved by the use of a stepper motor along with a lead screw. As seen in Figure 4.4.1.6, the tubes are mounted onto two wooden plates that are a distance of 17 cm apart. The wooden plates are secured onto one nut each. The motor is

mounted and secured onto the body of the machine. As the motor turns, the lead screw is free to turn while the nuts are not. Therefore, the revolution of the motor moves the tubes back and forth. In order to facilitate the movement of the tubes, or the wooden plates, the top frame of the machine must have the configuration as in 4.4.1.7.

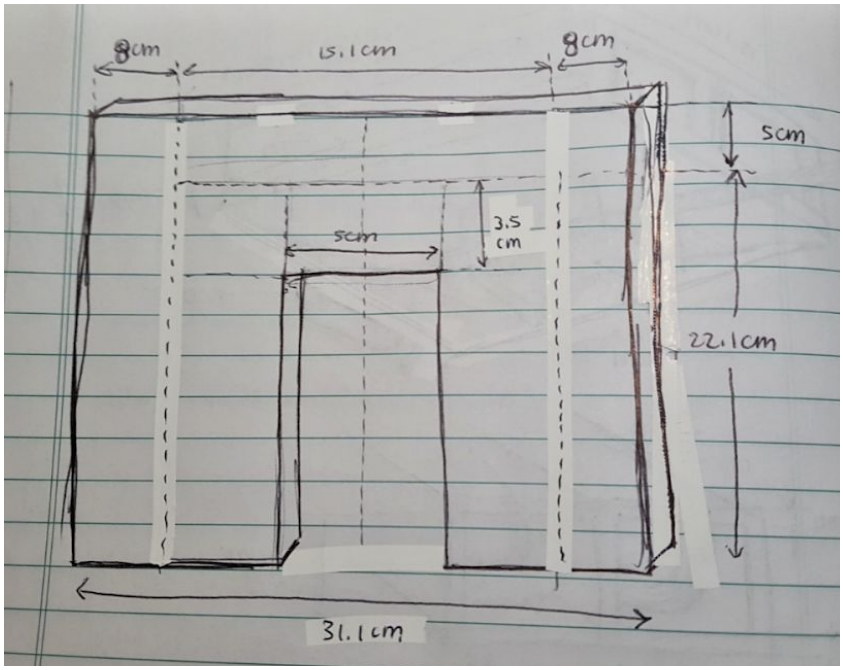

Figure 4.4.1.7. Top frame of the machine

Note that this mechanism extends and contracts both tubes at the same time, even though tires will only be deployed from one of the two tubes. This mechanism was chosen as it reduces the number of actuators and hence the overall cost.

Location of Sensors

This design uses two types of sensors: an ultrasonic sensor and an IR sensor. Two ultrasonic sensors are used to detect the presence of poles. As seen in Figure 4.4.1.8, each ultrasonic sensor will be positioned directly below each hook, at some distance within 11.5 cm from the ground up. Three IR sensors are used to detect the number of tires on a pole once a pole is detected. The bottom-most IR sensor detects the presence of the bottom-most tire, and the middle sensor detects the presence of the second tire. The third sensor detects whether or not the detections made by the bottom and middle sensors are valid; if the third sensor detects an obstruction, this means that the pole has been detected, rather than a tire.

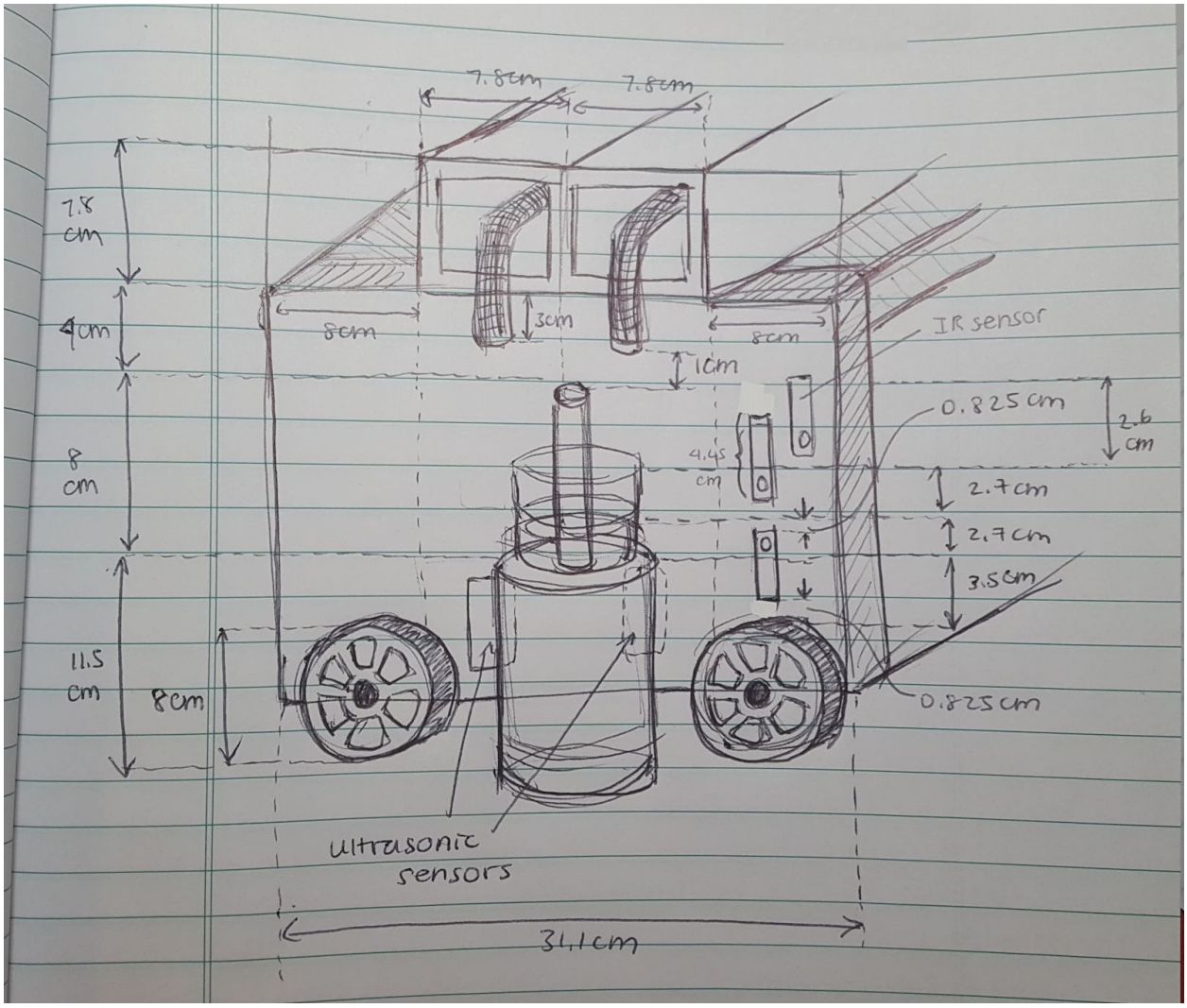

Figure 4.4.1.8. View of the side of the machine from which tires are deployed.

Driving Mechanism

A differential driving mechanism was chosen due to low cost, ease of implementation, and simplicity [1]. Due to the extension mechanism, our design solution does not require turning of any kind and must only go straight. A differential drive will allow our machine to drive straight by facilitating a mechanism for correcting any deviations that result from imprecise manufacturing, among other factors, by controlling the speed of each of the two back wheels.

Specification of Motors

There are a total of five motors used in the design solution. Two of these motors are used to deploy tires onto a pole by advancing the stack of tires by increments of the thickness of a tire every time. One motor is used to extend the tube of stacked tires forwards and backwards to account for the 10cm positional-variation of the poles. Two other motors are to be attached to the back wheels of the machine to facilitate a differential driving mechanism. The details of the torque and RPM requirements and other motor specifications required by each of the three

functions is outlined in Table 4.4.2.1. Refer to Appendix 8.1 for calculations on torque and RPM requirements.

Table 4.4.1.1. A summary of functions, their torque and RPM requirements, and other specifications

Function	Specifications	Torque (Nm)	RPM
Differential Driving	● High torque is required to overcome the machine's weight, but high speed is not required ● Differential driving is preferred over using a single motor to drive the machine's two back wheels. It is not necessary for our machine to turn, but a differential driving system makes it significantly easier to drive the machine straight. If cost or weight becomes a problem, the differential driving may be changed to use a single motor	0.32	9.54
Tube Extension	● Requires highly precise positioning. The motor must turn an exact number of revolutions so that the tube extends by precisely the amount needed for the hook to near the pole ● High speed is preferred	3.462×10^{-3}	342.6
Tire Advancement and Deployment	● Requires highly precise positioning. The motor must turn an exact number of revolutions so that the stack of tires increments by the thickness of one tire each time, to ensure that exactly one tire is deployed at a time ● High speed is preferred	2.19×10^{-3}	342.6

Stepper motors are ideal for precise positioning [18] and were thus chosen for the tube extension and tire advancement and deployment:

- Tube Extension: NEMA 17 Stepper Motor ($holding\ torque\ =\ 0.40\ Nm$ [19])
- Tire Advancement and Deployment: Nema 17 Stepper Motor ($holding\ torque\ =\ 0.40\ Nm$ [19])

The chosen stepper motors offer a higher torque than required, which justifies the choice of the motors.

Figure 4.4.1.9: NEMA 17 Stepper Motor

Due to the high torque and low speed requirement of the differential driving mechanism, a DC motor was chosen:

- Differential Driving: Shenzhen DC Motor ($at\ load\ torque = 0.120\ Nm,\ RPM = 50$) [20]

The 0.120 Nm-at-load-torque of the Shenzhen DC Motor is lower than the estimated torque requirement of 0.32 Nm. However, this prediction was based on the worst case scenario, with the mass prediction being 8 kg. If the prototype is built and the torque provided by two Shenzhen DC Motors is found to be insufficient, four motors will be used to drive the robot.

Figure 4.4.1.10: Shenzhen DC Motor

Wheels

Based on the availability of wheels made to accompany the Shenzhen DC Motor, the following plastic robot wheel was chosen (Figure 4.4.1.9).

Figure 4.4.1.11. Plastic robot wheel made to fit the Shenzhen DC Motor [21]

The tire has a diameter of 6.5 cm and thickness of 2.8 cm [21]. The diameter is less than the 8 cm value that was estimated in our calculation of torque. This is preferable, as a smaller radius reduces the torque required. If the team proceeds to use this wheel, some small adjustments to dimensions have to be made.

4.4.2 Circuit Design

This section describes circuit diagrams for the major components of the machine including the motors, sensors and pole detection indicator circuit. A brief discussion on power supply and emergency stop is also included.

Motors

Two types of motors - stepper motors for the extension and deployment mechanisms and and DC for the wheels - are being used as discussed previously.

NEMA 17 Stepper Motor:

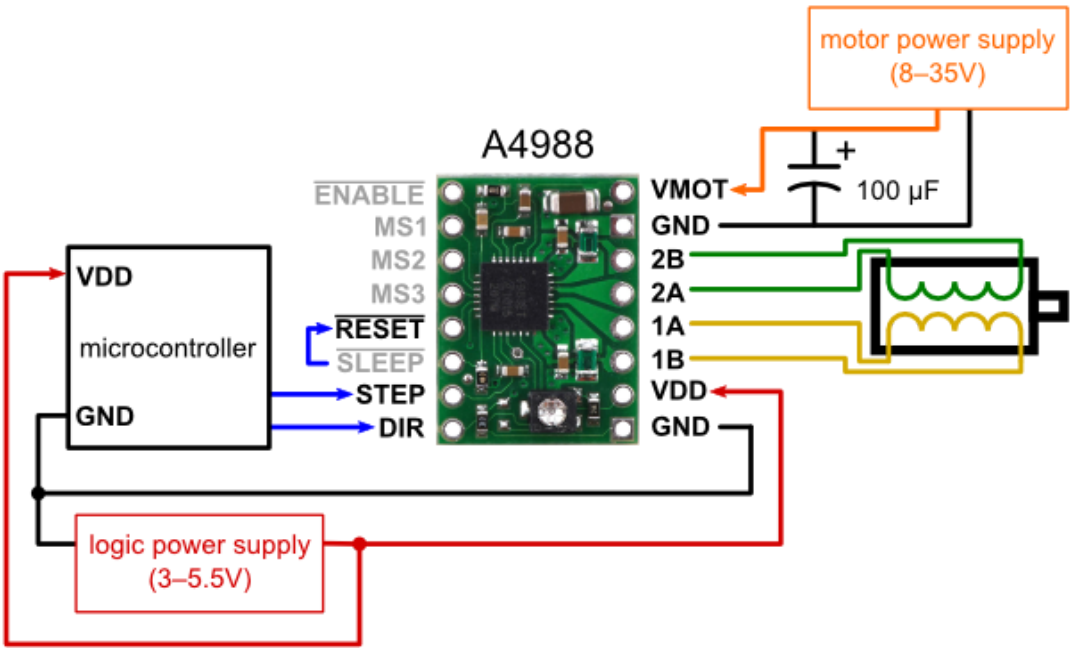

Figure 4.4.2.1: Circuit diagram for NEMA 17 Stepper Motor using A4988 driver board [22]

The NEMA 17 motor is a bipolar stepper motor which means that the supply voltage must be alternately applied to different coil ends [1]. It is controlled by the A4988 driver board. As can be seen in the circuit diagram above, both ends of the green and yellow coil are connected to the driver. Each coil pair requires an H-bridge and thus the A4988 is used (Figure 4.4.2.2).

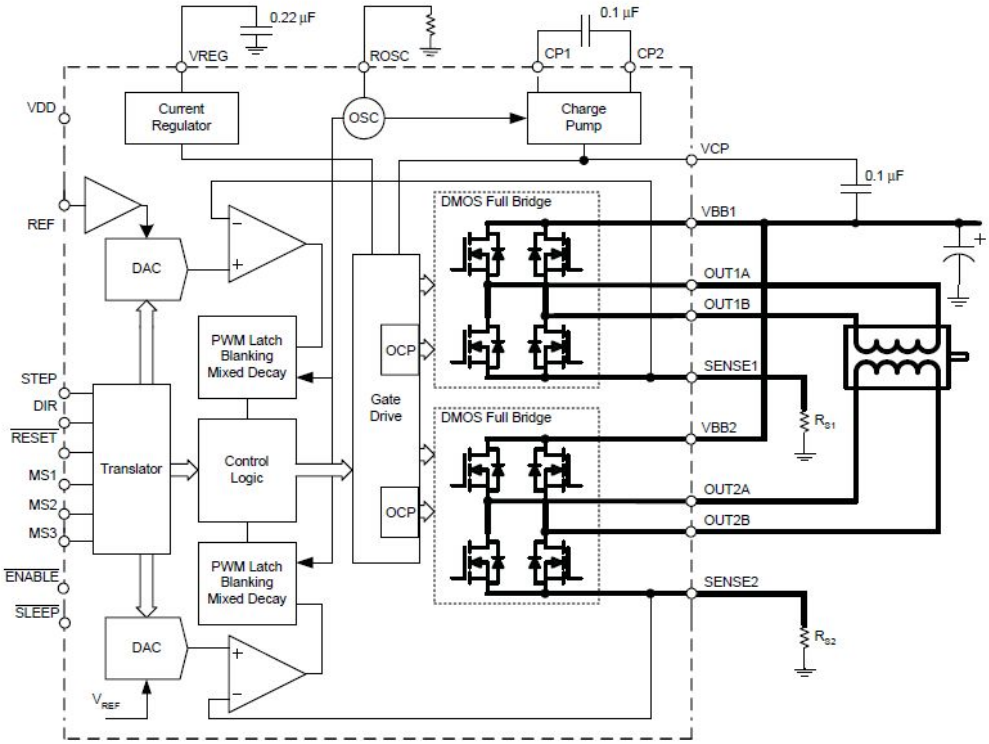

Figure 4.4.2.2: Internal Circuit of A988 indicating two H bridges (in bold) [23]

The driver can be powered by the microcontroller but since three stepper motors are on the machine, to minimise the number of pins utilised, the three motors will be connected to an external 3-5.5 V power supply. The STEP and DIR inputs receive signals from the microcontroller to control the microstep and direction of rotation respectively. Each pulse to the STEP input corresponds to a microstep in a direction selected by the DIR pin. The A4988 can provide higher step resolution than the typical 1.8° thus allowing for more precise movement - a feature necessary when extending till the exact variance distance and pushing off an exact amount of tires onto the poles. Further inputs to MS1, MS2, S3 determine the stepper driving modes according to the table below. [21]

Table 4.2.2.1: inputs to MS1, MS2, MS3 to change Stepper Driving Modes [24]

MS1	MS2	MS3	Microstep Resolution
Low	Low	Low	Full step
High	Low	Low	Half step
Low	High	Low	Quarter step
High	High	Low	Eighth step
High	High	High	Sixteenth step

The motor is connected to an external power supply of 8-35V. The board is susceptible to LC voltage spikes, especially when using wires greater than a few inches (which may be the case

for the machine). The 100 μF capacitor is attached to prevent voltage spikes greater than the maximum voltage rating of the board (35V) from damaging it.

Shenzhen DC Motor: Model TGP01S-A130 Gear Motor
The Shenzhen DC Motor requires a H-bridge circuit to control speed and direction. Speed is controlled using pulse width modulation i.e. changing the DC current on-off duration. Direction is controlled by changing the base voltage to the transistors. These differing signals come from the microcontroller as indicated by the 555 Timer circuit.

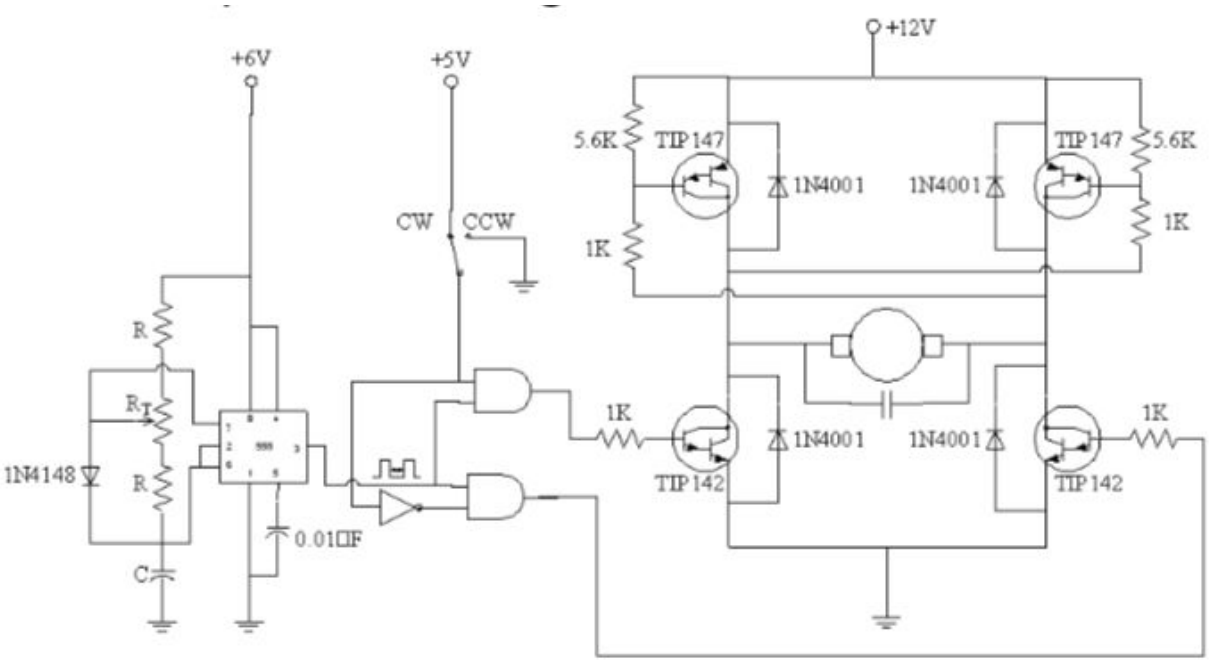

Figure 4.4.2.3: H-Bridge for Shenzhen DC Motor [25]

The basic principle is that PNP transistors (TIP147) switch off when base voltage is high while NPN (TIP142) switch on. The following table explains the different directions of motions and the signals applied to achieve them:

Table 4.4.2.3: Directional control of DC motor [25]

Upper Left TIP147	Upper Right TIP147	Lower Left TIP142	Lower Left TIP142	Direction
Off	Off	Off	Off	Off/Coast
On	Off	Off	On	FWD
Off	On	On	Off	RVS
On	On	Off	Off	Break

The 1KΩ resistors and diodes are added to protect circuit.

Sensors

HCR04 Ultrasonic Sensor

The HCR04 ultrasonic sensor is an inexpensive, compact and fairly accurate sensor with a range of detection large enough to cater to our needs for a maximum distance of 10cm. The figure below shows the circuit diagram of the sensor which will directly be connected to the PIC board by the TRIP (receiving external signal) and ECHO (transmitting output signal) I/Os [13]. The LM7805 voltage regulator drops the voltage from the 12V power supply (discussed later) to the required 5V. The capacitors are added to remove input and output noise.

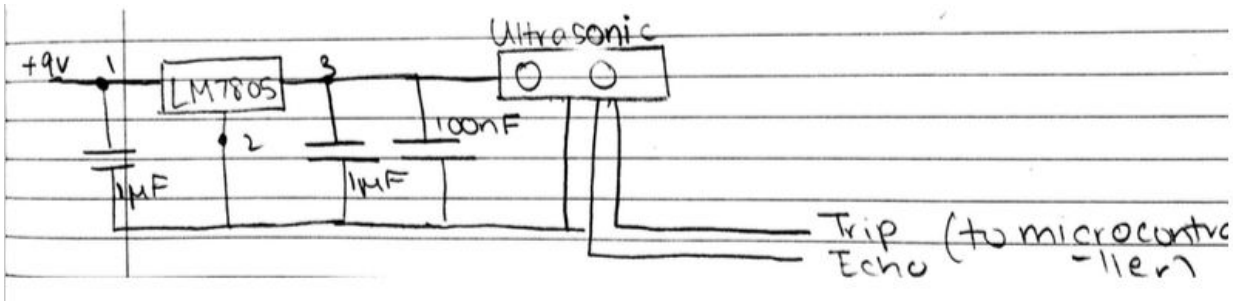

FIgure 4.4.2.4: Circuit Diagram for Ultrasonic Sensor [16]

SHARP GP2Y0A41SK0F Infrared Sensor

The SHARP GP2Y0A41SK0F Infrared Sensor is another inexpensive and accurate sensor. Both testing and datasheet figures show that this sensor is much more accurate than the ultrasonic sensor and is thus being used to detect the poles while the machine is in motion as well as detecting the number of tires on each pole. Another advantage over the ultrasonic sensor is that it only occupies a single pin on the microcontroller. This sensor will be controlled by the Arduino Nano. Again, as before the LM7805 voltage regulator is used to get the allowed voltage.

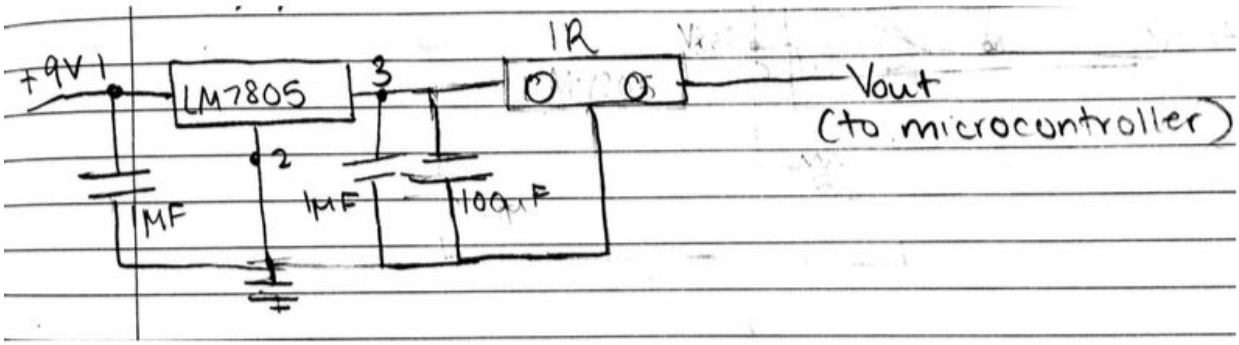

FIgure 4.4.2.5: Circuit Diagram for Infrared Sensor [16]

Pole Detection Indicator Circuit

The pole detection indicator circuit refers to the circuit that will create an indication (in the form of LEDs lighting up) when a pole is detected. The circuit utilises the LM339 Quad Op Amp Comparator connected to four LEDs [26] that light up when the input voltage i.e. IR sensor output is above a reference voltage. Thus, when the IR sensor detects a pole, the output voltage generated while light up this circuit. An important fact to note with this circuit is that the output voltage may not be stable and fluctuations from the reference voltage may give faulty readings. This confirmation and the actual use of this circuit can only be determined after testing.

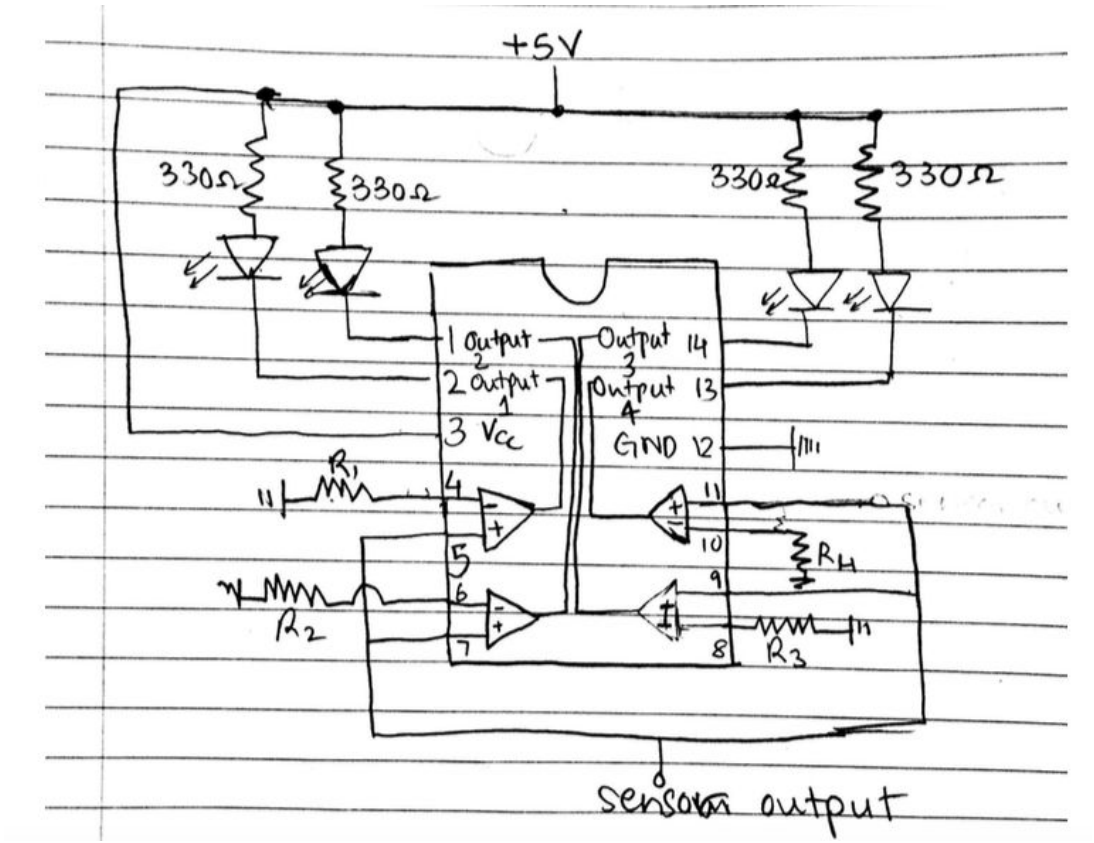

FIgure 4.4.2.6: Pole Detection Circuit Using LM339 Quad Op Amp Comparator [23]

Power Supply and Step Down Circuits

This section describes preliminary power calculations considering only the major power drawing components to get an idea about the kind of battery that could be utilised. Further, another decision to be made is whether a single power supply will be used or will there be different power supplies for different circuits e.g. one for DC motors, one for stepper etc. This decision will also determine the type of emergency stop that has to be enabled.

If a battery were to be used, it would most likely be a 12V, 60W DC battery - 12 V to account for the voltage needs of the stepper motors and 60W considering a factor of safety. This voltage will then be stepped down for the other components. An example of a voltage regulator circuit using the LM7805 voltage regulator had been shown with the sensor circuits in Figures 4.4.2.4 and 4.4.2.5.

Table 4.4.2.2: Power Calculations for major components

Component	Number	Voltage Rating	Current Rating
HCR04 Ultrasonic Sensor	2	5 V	15 mA
SHARP IR Sensor	3	5.5 V	33 mA
NEMA 17 Stepper Motor	3	12 V	0.4 A
AC4988 Driver Board	3	4.5 V	0.5 A
Shenzhen DC Motor	2	4.875 V	500 mA
Arduino Nano	1	5 V	19 mA
PIC Board	1	5.5 V	1 A
Power Required		38.627 W	

4.4.3 Microcontroller Design

Pin assignment

PIC18F4620 and develop board (Master)

Pin	Type	I/O	Description
RA0-RA1	Digital	Output	Control the driver of stepper motor in front tube. RA0: Step; RA1: Direction
RA2, RA5	Digital	Output	Control the driver of stepper motor in rare tube. RA2: Step; RA3: Direction
RA3-RA4	-	-	Leave for future analog or digital input
RA6-RA7	-	-	PIC; leave for future application
RB0, RB2,	Digital	Output	Control the driver of stepper motor in extension system. RB0: Step; RB2: Direction
RB1, RB4-7	-	-	Keypad control
RC0-RC1	Digital	Input	Each send a triggering signal to start each ultrasonic sensors
4	digit	in/out	2 ultrasonic
RC3-RC4			RTC
RD2-RD7			LCD
			Keypad

Arduino Nano (Slave)

Pin	Type	I/O	Description
A0, A1, A2	Analog	Input	Receiving distance data from IR proximity sensors
	Digital	Output	Control the driver of stepper motor in rare tube. RA2: Step; RA3: Direction
RA3-RA4	-	-	Leave for future analog or digital input

RA6-RA7	-	-	PIC
RB0, RB2,	Digital	Output	Control the driver of stepper motor in extension system. RB0: Step; RB2: Direction

Main program

main.c

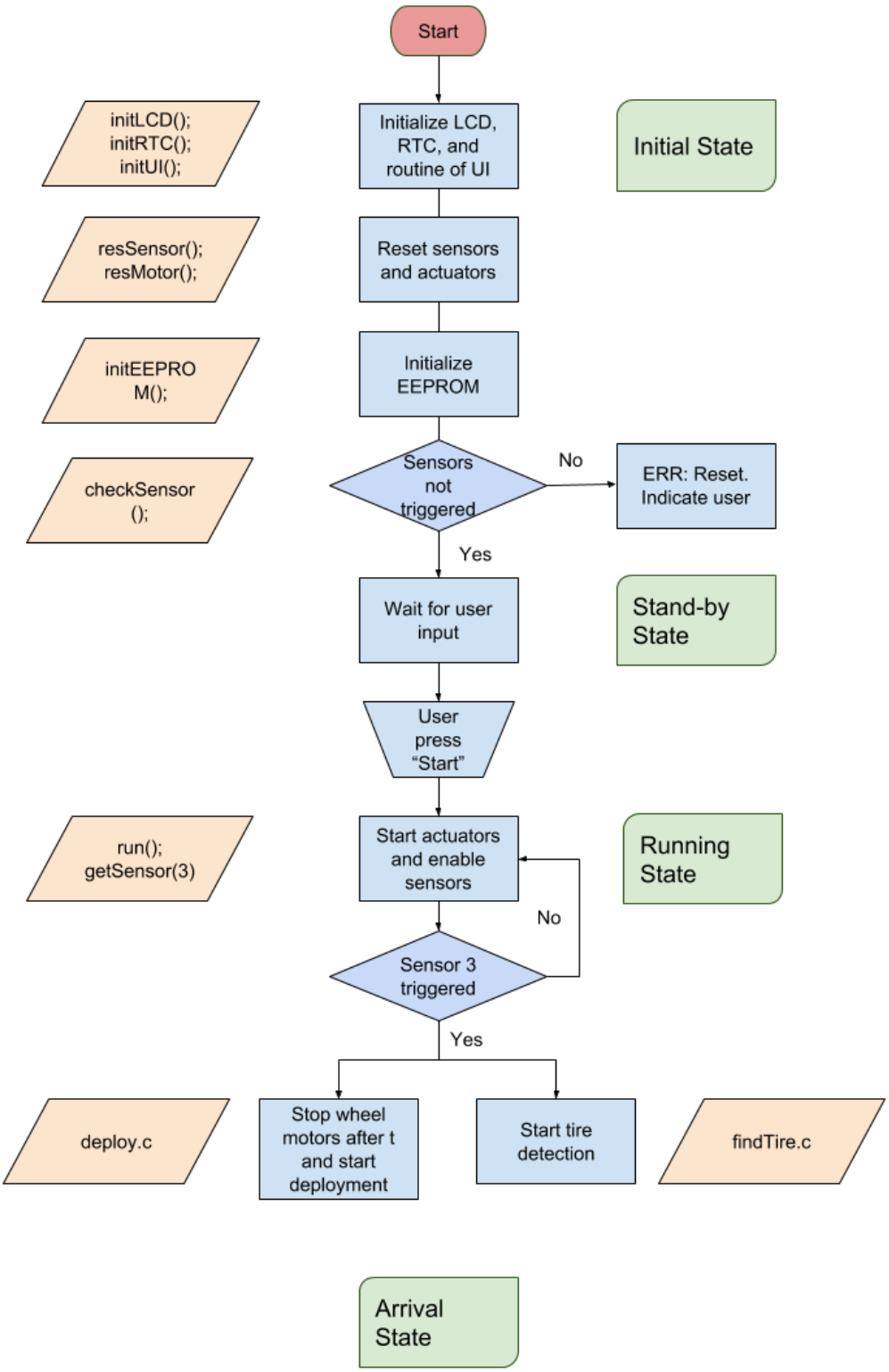

5 PROJECT MANAGEMENT

5.1 STATEMENT OF WORK

Electromechanical Engineer

Yewon is the Electromechanical Engineer and will be responsible for constructing the frame of the prototype, constructing various functional mechanisms, incorporating the actuators into the system, and acquiring the materials needed. Some of the key functional mechanisms that she will build include the tube extension mechanism, the tire advancing mechanism, and the differential driving mechanism. She will also be in charge of mounting the sensors in the correct locations on the machine so that the desired object is detected.

Electrical Engineer

Bipasha is the Circuits Engineer is responsible for designing and constructing all the circuitry for the machine to connect all the sensors and actuators to the microcontroller. Shaft encoding and pole and tire detection are the major sensory tasks. She will control actuators using driver boards but also create a circuit entirely from scratch. She will determine the power requirements of the machine and will acquire and provide the necessary supply and connections for the same. She will also create emergency stop circuits, circuits to indicate pole detection, and provide the wiring for the entire machine. She will also consider noise and signal interference to create optimal circuits.

Microcontroller Engineer

Yuqian is the Microcontroller Engineer who will be responsible for developing the control algorithm of the machine, developing and debugging code, and designing and programming the user interface. She will also develop some extra features of the machine including a real-time display. She will be using microcontroller development board and arduino nano to control the machine and develop algorithms in C. She will be in charge of correct tire and pole detection as well as sensor acquisition.

5.2 GANTT CHART

5.3 PERT CHART

5.4 BUDGETING

Category	Component	Amount	Single price (CAD$)	Total price (CAD$)
Sensor	Ultrasonic Distance Sensor HC-SR04	2	2.74	5.49
	IR proximity sensor 4-30cm GP2Y0A41SK0F	3	14.95	44.85
Motor	Shenzhen DC Gear Motor with tires (package)	2 Motors, 4 wheels	2.12	12.74
	Nano Nema 17 Stepper Motor	3	15.33	45.99
Drivers	A4988 stepper motor driver	3	1	3
Mechanical Components	Lead screw T8 300mm	3	1.94	5.82
	Shaft	2	1.20	2.40
	8cm diameter Wheel set of 4	1	14.30	14.30
Power	Battery (undecided)			
Electrical Components	LM339 Comparator	1	1 Home Hardware	1
	LM7805 Voltage Regulator	5	1.92	9.60

	TIP147 Transistor	4	1.51	6.04
	TIP142 Transistor	4	2.93	11.72
	IN4001 Diode	8	0.33	2.64
Microcontroller	PIC18F4602 + AER201 Develop board + LCD + keypad+RTC	1	67.00	67.00
	Arduino Nano	1	5	5
Total				237.59

Note: The cost is greater than the given constraint on cost i.e. $237 but this is mainly because least cost versions of the products have not been obtained.

6 CONCLUSION

The tire stacking machine being proposed will autonomously detect poles and stack a variable amount of tires on them depending on the number of tires already present on the poles and certain distance measurements of the poles from each other. This idea has potential use in the increasingly automated tire manufacturing and storage industry. Being a lightweight, compact, inexpensive and mobile machine, it already poses several advantages upon existing solutions to tire stacking and storage which are of industrial size, extremely expensive and fairly complex.

The proposed design can be broadly divided into three submodules: motion, detection, and deployment. Motion refers to the self regulated movement of the machine along a straight line besides the pole, detection refers to both detection of poles and tires and finally deployment refers to the actual transfer of tires from the machine to the poles. The proposed solution will use a differential drive system with DC motors to ensure straight line motion, employs ultrasonic and IR sensors for detection, and has a novel ‘tube and hook’ storage and extension system to accurately deploy tires on the poles.

The design can easily be scaled to hold more and larger tires. The program can be altered to deploy as many tires as one wants. Further this design could be extended to beyond tires and with a few modifications could be used to deploy other items.

Potential problems that the team could face while designing include inaccurate detection of poles and tires, imprecise stopping of the machine resulting in faulty deployment of tires, choppy motion of the extending and deployment system due to the use of stepper motors. Friction and lightweight of the tires has been a major concern while designing and this along with operation time can only be optimised through rigorous testing and modification. The goal, for now, is to meet the minimum functionality after which extra design features and optimisation will be considered. This will be done through constant and effective communication between subsystems with well defined roles for each. Advanced preparation and integration of subsystems allowing time for improvement and debugging is a requirement for a successful outcome.

7. REFERENCES

[1] M.R. Emami. Multidisciplinary Engineering Design: from theory to practice, 2019 Edition, 2019.

[2]: Smithers Rapra. The Future of Tire Manufacturing to 2022. [Online] Available: https://www.smithersrapra.com/market-reports/tire-industry-market-reports/the-future-of-tire-manufacturing-to-2022. Date Accessed: January 28th, 2019.

[3]: Freedonia. World Tires. [Online] Available: https://www.freedoniagroup.com/industry-study/world-tires-3357.htm. Date Accessed: January 28th, 2019.

[4]: Lubeck J., Tire Industry Automation: Now a Necessity. [Online] Available: https://www.laser-view.com/tire-industry-automation-necessity/ Date Accessed: January 28th, 2019.

[5]: SwissLog. Michelin Nordic, Sweden: Tire warehouse modernization [Online] Available:

https://www.swisslog.com/en-ca/logistics-automation/case-studies-and-resources/case-studies/2016/07/michelin-nordic Date Accessed: January 28th, 2019.

[]6: Lubeck J.,Thick vertical for High efficiency part storage. [Online] Available: https://www.laser-view.com/think-vertical-high-efficiency-part-storage-engineering-com/ Date Accessed: January 28th, 2019.

[7]: Zhang Y. AER201 Tire Stacking Machine. Champion 2011. [Online]. Available: https://www.youtube.com/watch?v=UyE1CIq3Db0&t=8s

[8]: Shi, H. University of Toronto AER201 Project Team 56. [Online]. Available: https://www.youtube.com/watch?v=Lv1YOnw0dIc&t=101s

[9]: McMahon M., Automotive Tire Stacking and Strapping Machine. [Online] Available: https://patents.google.com/patent/US3955491A/en Accessed: January 29th, 2019.

[10]: Thomas M. Raben. “US5562392A: Automated tire loading/unloading and compression system and tire transport frame.” 2000.

[11]: Thomas M. Raben. “US5562392A: Tire-stacking device and accessories for use in cooperative arrangement with a lift truck.” 1994.

[12]: Perneder R., Osborne I. (2011) Timing Belts in Linear Drives. In: Handbook Timing Belts. Springer, Berlin, Heidelberg. Access:https://link.springer.com/chapter/10.1007/978-3-642-17755-2_4

[13] Perneder, R. and Osborne, I. (2012). Timing Belts in Linear Drives. [online] Available at: https://link.springer.com/chapter/10.1007/978-3-642-17755-2_4 [Accessed 30 Jan. 2019].

[14]: HCSR04 Datasheet. [Online] Available: https://www.mpja.com/download/hc-sr04_ultrasonic_module_user_guidejohn.pdf

[15]: Sharp GP2Y0A41SK0F Datasheet: [Online] Available: https://www.pololu.com/file/0J713/GP2Y0A41SK0F.pdf Accessed: January 29th, 2019. Infrared Sensor (Sharp GP2Y0A41SK0F)

[16]: [Online] Available: http://robojax.com/learn/arduino/?vid=robojax-infrared-obstacle Date Accessed: January 28, 2019

[17]: Emami. R., Lecture Slides. [Online]. Available:https://q.utoronto.ca/courses/82084/modules Accessed January 25th 2019.

[18] M. K. Alam. “Complete Motor Guide for Robotics.” [Online] Available: https://www.hackster.io/taifur/complete-motor-guide-for-robotics-05d998 Date Accessed: January 29, 2019

[19] “NEMA17-AMT112S Stepper Servo Motor.” Cui INC. Available: https://www.cui.com/product/resource/nema17-amt112s.pdf Date Accessed: January 28, 2019

[20] Shenzhen DC Motor, Model: TGP01S-A230 Gear Motor. [Online] Available: https://q.utoronto.ca/courses/82084/files/837663?module_item_id=479469D ate Accessed: January 28, 2019

[21] “DC 3V 110RPM Gear Motor Smart Car Robot Plastic Tire Wheel”. [Online] Available: https://www.amazon.ca/Yosoo-Smart-Robot-Wheel-Arduino/dp/B019OH4GHC/ref=sr_1_33?ie=UTF8&qid=1548826634&sr=8-33&keywords=plastic+toy+car+tire+wheel Date Accessed: January 29, 2019.

[22]: Pololu. A4988. [Online] Available:https://www.pololu.com/product/1182. Accessed: January 29th, 2019.

[23]: Allegro Microsystems. A4988: DMOS Microstepping Driver with Translator and Overcurrent Protection. [Online] Available: https://www.allegromicro.com/en/Products/Motor-Driver-And-Interface-ICs/Bipolar-Stepper-Motor-Drivers/A4988.aspx. Accessed: January 29th, 2019.

[24]: Unknown. My experiments with stepper motor. [Online] Available: https://scientistnobee.wordpress.com/2015/03/12/my-experiments-with-stepper-motor/ Accessed: January 29th, 2019.

[25]: AER201:Engineering Design.Circuits and Sensors. [Online] Available: https://q.utoronto.ca/courses/82084/files/2389006?module_item_id=521897 Accessed: January 26th, 2019.

[26] Learning About Electronics. How to Build an LM339 Quad Voltage Comparator Circuit [Online] Available:http://www.learningaboutelectronics.com/Articles/LM339-quad-voltage-comparator-circuit.php .Accessed: January 29th, 2019.

8 APPENDICES

8.1 NUMERICAL DATA FROM ULTRASONIC SENSOR TEST

	Distance from centerline of base (cm) (where -4 is the radius of the base and thus value (-4) is the actual distance seen by sensor)					
Sensor	10 (-4)	12 (-4)	14 (-4)	16 (-4)	18 (-4)	20 (-4)
Ultrasonic	7.265	10.239	11.761	17.188	19.684	20.342
	6.889	10.0768	11.111	14.068	18.256	20.803
	6.735	10.496	11.692	14.068	19.282	21.53
Average	6.963	10.2706	11.52133333	15.108	19.074	20.89166667

8.2 AHP FOR REMAINING SUBSYSTEMS

Deployment Mechanism

Precise Movement RP Matrix					Normalized Precise Movement RP Matrix					Overall Preference
	Tube & Hook	Conveyor Belt	Trap Door	Fork-lift		Fork-lift	Tube & Hook	Trap Door	Conveyor Belt	
Tube & Hook	1	5	4	1/7	Fork-lift	0.118	0.294	0.276	0.105	0.198
Conveyor Belt	1/5	1	½	1/9	Tube & Hook	0.024	0.059	0.034	0.081	0.05
Trap Door	1/4	2	1	1/9	Trap Door	0.03	0.118	0.069	0.081	0.074
Fork-lift	7	9	9	1	Conveyor Belt	0.828	0.529	0.621	0.733	0.678

Manufacturability RP Matrix					Normalized Manufacturability RP Matrix					Overall Preference
	Tube & Hook	Conveyor Belt	Trap Door	Fork-lift		Tube & Hook	Conveyor Belt	Trap Door	Fork-lift	
Tube & Hook	1	3	5	8	Tube & Hook	0.603	0.643	0.606	0.421	0.568
Conveyor Belt	1/3	1	2	6	Conveyor Belt	0.201	0.214	0.242	0.316	0.243
Trap Door	1/5	1/2	1	4	Trap Door	0.121	0.107	0.121	0.211	0.14
Fork-lift	1/8	1/6	¼	1	Fork-lift	0.075	0.036	0.03	0.053	0.049

Reliability RP Matrix					Normalized Reliability RP Matrix					Overall Preference
	Tube & Hook	Conveyor Belt	Trap Door	Fork-lift		Tube & Hook	Conveyor Belt	Fork-lift	Trap Door	
Tube & Hook	1	4	7	4	Tube & Hook	0.609	0.615	0.583	0.615	0.606
Conveyor Belt	1/4	1	2	1	Conveyor Belt	0.152	0.154	0.167	0.154	0.157
Trap Door	1/7	1/2	1	1/2	Fork-lift	0.087	0.077	0.083	0.077	0.081
Fork-lift	1/4	1	2	1	Trap Door	0.152	0.154	0.167	0.154	0.157

Efficiency RP Matrix					Normalized Efficiency RP Matrix					Overall Preference
	Tube & Hook	Conveyor Belt	Trap Door	Fork-lift		Trap Door	Conveyor Belt	Fork-lift	Tube & Hook	
Tube & Hook	1	1/5	1/9	1/2	Trap Door	0.059	0.027	0.079	0.034	0.05
Conveyor Belt	5	1	1/6	5	Conveyor Belt	0.294	0.135	0.119	0.345	0.223
Trap Door	9	6	1	8	Fork-lift	0.529	0.811	0.713	0.552	0.651
Fork-lift	2	1/5	1/8	1	Tube & Hook	0.118	0.027	0.089	0.069	0.076

Cost RP Matrix					Normalized RP Matrix Deployment					Overall Preference
	Tube & Hook	Conveyor Belt	Trap Door	Fork-lift		Tube & Hook	Conveyor Belt	Trap Door	Fork-lift	
Tube & Hook	1	5	6	9	Tube & Hook	0.677	0.755	0.656	0.36	0.642
Conveyor Belt	1/5	1	2	4	Conveyor Belt	0.135	0.151	0.219	0.32	0.18
Trap Door	1/6	1/2	1	4	Trap Door	0.113	0.075	0.109	0.28	0.129
Fork-lift	1/9	1/4	1/4	1	Fork-lift	0.075	0.019	0.016	0.04	0.049

Objective RI Matrix					
	Precision	Manufacturability	Reliability	Efficiency	Cost
Precision	1	2	3	4	5
Manufacturability	0.5	1	2	3	4
Reliability	0.333	0.5	1	2	3
Efficiency	0.25	0.333	0.5	1	2
Cost	0.2	0.25	0.333	0.5	1

Normalized Objective RI Matrix						Overall Preference
	Precision	Manufacturability	Reliability	Efficiency	Cost	
Precision	0.438	0.49	0.439	0.381	0.333	0.416
Manufacturability	0.219	0.245	0.293	0.286	0.267	0.262
Reliability	0.146	0.122	0.146	0.19	0.2	0.161
Efficiency	0.11	0.082	0.073	0.095	0.133	0.099
Cost	0.088	0.061	0.049	0.048	0.067	0.063

Total Preference	
Tube & Hook	**0.374**
Conveyor Belt	0.143
Trap Door	0.153
Fork-lift	0.331
Tube & Hook wins!	

Matrix	Consistency Index	Consistency Ratio
Precision	0.08	0.02
Manufacturability	0.03	0.006
Reliability	0	0
Efficiency	0.08	0.02
Cost	0.05	0.009
Objective	-0.49	-0.109

Extension Mechanism

Manufacturability RP Matrix					Normalized Manufacturability RP Matrix					Overall Preference
	Lead screw	Linear Motion Rail/Draw	Rack & Pinion	Telescope & Timing Belt		Lead screw	Linear Motion Rail/Draw	Rack & Pinion	Telescope & Timing Belt	
Lead screw	1	2	6	8	Lead screw	0.558	0.585	0.536	0.4	0.52
Linear Motion Rail/Draw	1/2	1	4	6	Linear Motion Rail/Draw	0.279	0.293	0.357	0.3	0.307
Rack & Pinion	1/6	1/4	1	5	Rack & Pinion	0.093	0.073	0.089	0.25	0.126
Telescope & Timing Belt	1/8	1/6	1/5	1	Telescope & Timing Belt	0.07	0.049	0.018	0.05	0.047

Cost RP Matrix					Normalized Cost RP Matrix					Overall Preference
	Lead screw	Linear Motion Rail/Draw	Rack & Pinion	Telescope & Timing Belt		Lead screw	Linear Motion Rail/Draw	Rack & Pinion	Telescope & Timing Belt	
Lead screw	1	2	3	6	Lead screw	0.5	0.533	0.474	0.429	0.484
Linear Motion Rail/Draw	1/2	1	2	4	Linear Motion Rail/Draw	0.25	0.267	0.316	0.286	0.28
Rack & Pinion	1/3	1/2	1	3	Rack & Pinion	0.167	0.133	0.158	0.214	0.168
Telescope & Timing Belt	1/6	1/4	1/3	1	Telescope & Timing Belt	0.083	0.067	0.053	0.071	0.069

Objective RI Matrix			Normalized Objective RI Matrix			Overall Preference
	Cost	Manufacturability		Cost	Manufacturability	
Cost	1	0.25	Cost	0.2	0.2	0.2
Manufacturability	4	1	Manufacturability	0.8	0.8	0.8

Total Preference	
Lead screw	**0.491**
Linear Motion Rail/Draw	0.285
Rack & Pinion	0.160
Telescope & Timing Belt	0.065
Lead screw wins!	

Matrix	Consistency Index	Consistency Ratio
Cost	-0.99	-0.188
Manufacturability	-1	-0.188
RI	-1	-0.877

Sensors

Accuracy RP Matrix				Normalized Accuracy RP Matrix				Overall Preference
	Ultrasonic	IR proximity	IR Obstacle		IR proximity	Ultrasonic	IR obstacle	
Ultrasonic	1	1/2	5	IR proximity	0.313	0.31	0.333	0.319
IR proximity	2	1	9	Ultrasonic	0.625	0.621	0.6	0.615
IR obstacle	1/5	1/9	1	IR obstacle	0.063	0.069	0.067	0.066

Cost RP Matrix				Normalized Cost RP Matrix				Overall Preference
	Ultrasonic	IR proximity	IR obstacle		IR proximity	Ultrasonic	IR obstacle	
Ultrasonic	1	3	1/2	IR obstacle	0.3	0.231	0.31	0.28
IR proximity	1/3	1	1/9	Ultrasonic	0.1	0.077	0.069	0.082
IR obstacle	2	9	1	IR proximity	0.6	0.692	0.621	0.638

Objective RI Matrix			Objective RI Matrix			Overall Preference
	Accuracy	Cost		Accuracy	Cost	
Accuracy	1	5	Accuracy	0.833	0.833	0.833
Cost	1/5	1	Cost	0.167	0.167	0.167

Total Preference	
Ultrasonic	0.312
IR proximity	**0.526**
IR obstacle	0.162
IR proximity wins!	

Matrix	Consistency Index	Consistency Ratio
Accuracy	-1.00	-0.188
Cost	-1	-0.189

Drive Systems

Cost RP Matrix					Normalized Cost RP Matrix					Overall Preference
	Differential	Ackerman	Omni Wheel	Legged Robot		Differential	Ackerman	Omni Wheel	Legged Robot	
Differential	1	3	4	9	Differential	0.59	0.651	0.563	0.321	0.531
Ackerman Drive	1/3	1	2	9	Ackerman	0.197	0.217	0.281	0.321	0.254
Omni Wheel	1/4	1/2	1	9	Omni Wheel	0.148	0.108	0.141	0.321	0.18
Legged Robot	1/9	1/9	1/9	1	Legged Robot	0.066	0.024	0.016	0.036	0.035

Manufacturability RP Matrix					Normalized Manufacturability RP Matrix					Overall Preference
	Differential	Ackerman	Omni Wheel	Legged Robot		Differential	Ackerman	Omni Wheel	Legged Robot	
Differential	1	3	2	9	Differential	0.514	0.422	0.581	0.321	0.46
Omni Wheel	1/3	1	1/3	9	Omni Wheel	0.171	0.141	0.097	0.321	0.183
Ackerman	1/2	3	1	9	Ackerman	0.257	0.422	0.29	0.321	0.323
Legged Robot	1/9	1/9	1/9	1	Legged Robot	0.057	0.016	0.032	0.036	0.035

Objective RI Matrix			Normalized Objective RI Matrix			Overall Preference
	Cost	Manufacturability		Cost	Manufacturability	
Cost	1	0.25	Cost	0.2	0.2	0.2
Manufacturability	4	1	Manufacturability	0.8	0.8	0.8

Total Preference	
Differential	**0.474**
Ackerman Drive	0.197
Omni Wheel	0.294
Legged Robot	0.035
Differential wins!	

Matrix	Consistency Index	Consistency Ratio
Cost	-0.99	-0.19
Manufacturability	-1	-0.18
RI	-1	-0.877

8.3 CALCULATIONS FOR MOTOR SELECTION

8.3.1 Differential Driving

Torque

In order to calculate the torque required for the wheels to roll without slipping, the following assumptions are made.

a. The radius of the wheels is $r = 4\ cm$
b. The load carried by each of the two wheels driven by motors is $m = 4\ kg$
c. The machine must roll a total distance of 4m from the Start Line to the last pole and come back within 3 minutes
d. There are a total of 10 poles and they are equally spaced. This translates to a total of 10 stops that the motor has to make
e. The last 1 minute of 3 minutes is allocated for the machine to return to the Start Line

After each stop, the motor must accelerate from zero velocity in order to reach the next pole. This acceleration can be modeled using the following kinematic equation:

$$d = \tfrac{1}{2}at^2 .$$

To solve for acceleration a, d and t must be known. Assumptions (c) and (d) imply that the machine has a maximum of 12 seconds to spend to move from one pole to the next and deploy tires onto the next pole, and that there is 40 cm between two consecutive stops. Thus, it is realistic to assume that the time taken to accelerate to a is $t = 2\ s$ over a distance $d = 4\ cm$. This gives $a = 0.02\ m/s^2$.

The force F applied by the wheel son the ground is given by

$$F = \tau / r$$

where τ is the torque and $F = ma$. Solving for the torque with $m = 4\ kg$ (assumption (b)), $r = 4\ cm$ (assumption (a)), and $a = 0.02\ m/s^2$ yields $\tau = 0.32\ Ncm$.

RPM or Angular Velocity

The velocity v of the machine and the angular velocity ω of the machine are related by

$$v = r\omega \text{ or } \omega = v/r .$$

Our velocity $v = at = (0.02)(2) = 0.04\ m/s$ and radius $r = 4\ cm$ yields $\omega = 1\ rad/s = 9.54\ RPM$.

8.3.2 Tire Advancer

RPM or Angular Velocity

A typical lead screw has 200 steps per revolution with 1 revolution corresponding to the nut traveling a distance of approximately $0.7\ cm$. Assuming that the desired speed is $v = 4\ cm/s$, the corresponding RPM is found as

$$\omega = 4\ cm/s \times 1\ rev/0.7cm \times 60s/min = 342.6\ RPM = 35.9\ rad/s$$

Torque

The torque that the motor must supply is a sum of torques from two sources. First, there is the torque required to turn the lead screw. Second, there is the torque due to the frictional force between the nut and the turning lead screw. That is,

$$\tau = I\alpha + F_{fr}r$$

Assuming that the lead screw is a cylinder of diameter $D = 0.7\ cm$ and length $L = 23\ cm$, and that it is made of steel with density $\rho = 7870\ kg/m^3$, the torque arising from turning the lead screw is

$$\tau_{lead\ screw} = I\alpha = (\tfrac{1}{2}mD^2/4)\ \alpha = \tfrac{1}{2}(\tfrac{\pi}{4}D^2L\rho)(D^2/4)\alpha$$

Assuming that the time taken to accelerate the motor to $\omega = 35.9\ rad/s$ is $1.5s$, we can find the angular acceleration as $\alpha = (35.9\ rad/s)/(1.5s) = 23.9\ rad/s^2$. Subsequently, $\tau_{lead\ screw} = 1.021 \times 10^{-3} Nm.$

To find the force of friction between the nut and the lead screw, the normal force between the nut and lead screw needs to be found. For simplicity, this normal force is taken to be the frictional force between the platform that is attached to the nut and the tube through which the platform moves. Assuming that the platform is made of ABS plastic with mass $m = 12.7g$, this normal (or force of friction) is found as $1.0923N$. Hence, the force of friction between the nut and lead screw is

$$F_{fr} = \mu_k N = (0.57)(1.0923) = 0.35 \times 10^{-2} N$$

Hence, the torque due to friction is

$$\tau_{fr} = F_{fr}r = (0.35 \times 10^{-2})(0.35 \times 10^{-2}) = 2.179 \times 10^{-3}\ .$$

Therefore,

$$\tau = \tau_{lead\ screw} + \tau_{fr} = 2.19 \times 10^{-3} Nm.$$

8.3.3 Tube Extender

RPM or Angular Velocity

Based on the same assumptions and calculations as Section 8.2.2, we obtain

$$\omega = 342.6\ RPM = 35.9\ rad/s\ .$$

Torque

The same calculation method is utilized as in Section 8.2.2, but with different values. The calculation will not be reproduced here, but it yields $\tau = 3.462 \times 10^{-3} Nm$.

8.4 DATA SHEETS FOR MOTORS

Shenzhen DC Motor: Model TGP01S-A130 Gear Motor
[]:Shenzhen DC Motor: Model TGP01S-A130 Gear Motor Datasheet [Online] Available: https://q.utoronto.ca/courses/82084/files/837663?module_item_id=479469 Accessed: January 29th, 2019.

Model：TGP01S-A130
Gear Motor

Applications
Description
Reduction Ratio:
1/48,、1/120、1/180、1/220、1/256、1/288

Weight：35g Unit：mm

MODEL		VOLTAGE		NO LOAD		AT LOAD					STALL		
		OPERATING RANGE	NOMINAL V	SPEED rpm	CURRENT A	SPEED rpm	CURRENT A	TORQUE N.m	TORQUE Kg.cm	OUTPUT w	TORQUE N.m	TORQUE Kg.cm	CURRENT A
TGP01S-A130	14150-120	3.0-12.0	4.5	100	0.20	87	0.50	0.066	0.675	0.40	0.265	2.700	1.25
	18100-220	3.0-12.0	3.0	50	0.20	40	0.60	0.120	1.233	0.6	0.393	4.003	2.15

Stepper Motor (NEMA 17)
[]: NEMA17 Stepper Motor Datasheet: [Online]
Available:https://www.cui.com/product/resource/nema17-amt112s.pdf Accessed: January 29th, 2019.

For more information, please visit the product page.

CUI INC®

date 06/26/2018
page 1 of 7

SERIES: NEMA17-AMT112S | **DESCRIPTION:** STEPPER SERVO MOTOR

FEATURES

- CUI AMT112S encoder + LIN Engineering stepper motor
- stepper motor with encoder for closed-loop mode when paired with a controller
- small, compact NEMA 17 frame size
- up to 110 oz-in (0.77 N-m) holding torque
- patented capacitive encoder ASIC technology
- incremental resolutions up to 4096 PPR
- resolutions programmable with AMT Viewpoint™ PC software
- digitally set zero position

IN PARTNERSHIP WITH
LIN ENGINEERING
The Step Motor Specialists
BACKED BY MOONS'

RoHS CE

MODEL	step angle (°)	current/ phase (A)	resistance/ phase typ (Ω±10%)	inductance /phase typ (mH±20%)	max holding torque (oz-in)	max optimal speed (RPS)	body length max (inch)
NEMA17-13-04SD-AMT112S	1.8	0.67	9.9	12.52	42.0	6	1.34
NEMA17-13-04PD-AMT112S	1.8	1.33	2.5	3.09	42.0	11	1.34
NEMA17-16-06SD-AMT112S	1.8	0.70	10.8	21.84	63.0	3	1.58
NEMA17-16-06PD-AMT112S	1.8	1.40	2.7	5.46	63.0	6	1.58
NEMA17-19-07SD-AMT112S	1.8	2.10	1.3	9.36	83.0	5	1.89
NEMA17-19-07PD-AMT112S	1.8	1.05	5.2	2.34	83.0	5	1.89
NEMA17-23-01D-AMT112S	1.8	2.00	2.0	2.91	110.0	7	2.34

8.5 DATA SHEETS FOR SENSORS

[]: Sharp GP2Y0A41SK0F Datasheet: [Online] Available: https://www.pololu.com/file/0J713/GP2Y0A41SK0F.pdf Accessed: January 29th, 2019.
Infrared Sensor (Sharp GP2Y0A41SK0F)

GP2Y0A41SK0F

Distance Measuring Sensor Unit
Measuring distance : 4 to 30 cm
Analog output type

■Description

GP2Y0A41SK0F is a distance measuring sensor unit, composed of an integrated combination of PSD (position sensitive detector), IR-LED (infrared emitting diode) and signal processing circuit.
The variety of the reflectivity of the object, the environmental temperature and the operating duration are not influenced easily to the distance detection because of adopting the triangulation method.
This device outputs the voltage corresponding to the detection distance. So this sensor can also be used as a proximity sensor.

■Agency approvals/Compliance

1. Compliant with RoHS directive (2002/95/EC)

■Applications

1. Cleaning robot
2. Personal robot
3. Sanitary

■Features

1. Distance measuring sensor is united with PSD, infrared LED and signal processing circuit
2. Short measuring cycle (16.5ms)
3. Distance measuring range : 4 to 30 cm
4. Package size (29.5 × 13.0 × 13.5mm)
5. Analog output type

■Absolute maximum ratings

(Ta=25°C, Vcc=5V)

Parameter	Symbol	Ratings	Unit	Remark
Supply voltage	Vcc	-0.3 to +7	V	-
Output terminal voltage	Vo	-0.3 to Vcc+0.3	V	-
Operating temperature	Topr	-10 to +60	°C	-
Storage temperature	Tstg	-40 to +70	°C	-

■Operating supply voltage

Symbol	Rating	Unit	Remark
Vcc	4.5 to 5.5	V	-

■Electro-optical Characteristics

Parameter	Symbol	Conditions	MIN.	TYP.	MAX.	Unit
Measuring distance range	ΔL	(Note 1)	4	-	30	Cm
Output terminal voltage	Vo	L=30cm (Note 1)	0.25	0.4	0.55	V
Output voltage difference	ΔVo	Output change at L change (30cm → 4cm) (Note 1)	1.95	2.25	2.55	V
Average supply current	Icc	L=30cm (Note 1)	-	12	22	mA

※L : Distance to reflective object

(Note 1) Using reflective object : White paper

(Made by Kodak Co., Ltd. gray cards R-27・white face, reflective ratio ; 90%)

■Timing Chart

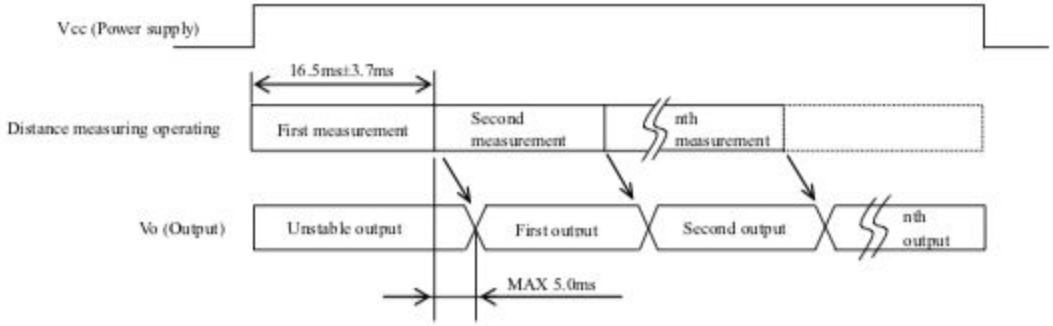

Ultrasonic Sensor (HC-SR04)

[]: HC-SR04 Datasheet: [Online] Available: https://www.mpja.com/download/hc-sr04_ultrasonic_module_user_guidejohn.pdf Accessed: January 29th, 2019.

3. Product Views

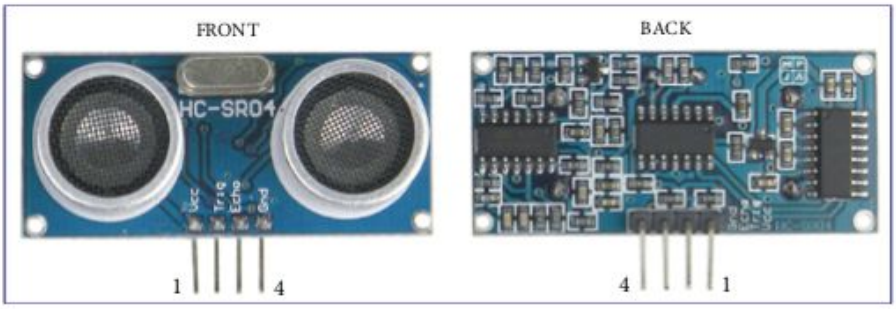

4. Module Pin Asignments

	Pin Symbol	Pin Function Description
1	VCC	5V power supply
2	Trig	Trigger Input pin
3	Echo	Receiver Output pin
4	GND	Power ground

5. Electrical Specifications

WARARNING
Do Not connect Module with Power Applied! Always apply power after connecting Connect "GND" Terminal first

Electrical Parameters	HC-SR04 Ultrasonic Module
Operating Voltage	5VDC
Operating Current	15mA
Operating Frequency	40KHz
Max. Range	4m
Nearest Range	2cm
Measuring Angle	15 Degrees
Input Trigger Signal	10us min. TTL pulse
Output Echo Signal	TTL level signal, proportional to distance
Board Dimensions	1-13/16" X 13/16" X 5/8"
Board Connections	4 X 0.1" Pitch Right Angle Header Pins

AMT112S ENCODER

ELECTRICAL

parameter	conditions/description	min	typ	max	units
power supply	VDD	4.5	5	5.5	V
start up time			200		ms
current consumption	with unloaded output		16		mA
output high level		VDD-0.1			V
output low level				0.1	V
output current (per channel)				15	mA
rise/fall time			8		ns

INCREMENTAL CHARACTERISTICS

parameter	conditions/description	min	typ	max	units
channels	CMOS Voltage: A, B, Z				
waveform	CMOS voltage square wave				
phase difference	A leads B for CCW rotation (viewed from front)				
quadrature resolutions[1]	48, 96, 100, 125, 192, 200, 250, 256, 360, 384, 400, 500, 512, 768, 800, 1000, 1024, 1600, 2000, 2048, 2500, 4096				PPR
index[2]	one pulse per 360 degree rotation				
accuracy			0.2		degrees
quadrature duty cycle			50		%

Notes: 1. Resolution programmed with AMT Viewpoint™ PC software. Default resolution set to 400 PPR.
2. Zero position alignment set with AMT One Touch Zero™ module, AMT Viewpoint™ PC software, or serial commands

MECHANICAL

parameter	conditions/description	min	typ	max	units
weight			15.7		g
rotational speed (at each resolution)	48, 96, 100, 125, 192, 200, 250, 256, 384, 400, 500, 512, 800, 1000, 1024, 2048			8000	RPM
	360, 768, 1600, 2000, 4096			4000	RPM
	2500			2500	RPM

ENCODER WAVEFORMS

Figure 1

Quadrature signals with index showing counter-clockwise rotation

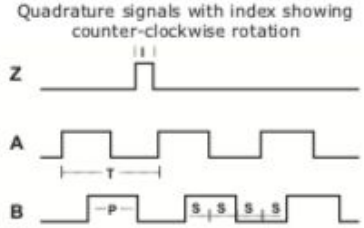

The following parameters are defined by the resolution selected for each encoder, where R = resolution.

Parameter	Description	Expression	Units
T	period	360/R	mechanical degrees
P	pulse width	T/2	mechanical degrees
I	index width	P/2	mechanical degrees
S	A/B state width	P/2	mechanical degrees

8.6 DATA SHEETS FOR MICROCONTROLLERS

Microcontroller
Arduino Nano
[]: Arduino Nano. [Online] Available: HC-SR04 Datasheet: [Online] Available: https://www.mpja.com/download/hc-sr04_ultrasonic_module_user_guidejohn.pdf Accessed: January 29th, 2019. Accessed: January 29th, 2019.

OVERVIEW | TECH SPECS | DOCUMENTATION

Microcontroller	ATmega328
Architecture	AVR
Operating Voltage	5 V
Flash Memory	32 KB of which 2 KB used by bootloader
SRAM	2 KB
Clock Speed	16 MHz
Analog IN Pins	8
EEPROM	1 KB
DC Current per I/O Pins	40 mA (I/O Pins)
Input Voltage	7-12 V
Digital I/O Pins	22 (6 of which are PWM)
PWM Output	6
Power Consumption	19 mA
PCB Size	18 x 45 mm
Weight	7 g
Product Code	A000005

8.7 DATA SHEETS FOR DRIVER BOARD

Driver Board
A4988 Driver Board
[A4988 Driver Board Datasheet: [Online]
Available:https://www.pololu.com/product/1182/specsAccessed: January 29th, 2019.

A4988 Stepper Motor Driver Carrier

Pololu item #: 1182 — 0 in stock
Brand: Pololu
Status: Active and Preferred
Free add-on shipping in USA
Free shipping in USA over $40

Price break	Unit price (US$)
1	5.95
5	4.95
25	4.49
100	3.95

Quantity: 1 — Backorder — *backorders allowed* — Add to wish list

This breakout board for Allegro's A4988 microstepping bipolar stepper motor driver features adjustable current limiting, over-current and over a heat sink or forced air flow (it is rated for 2 A per coil with sufficient additional cooling). This board ships with 0.1" male header pins included

Alternatives available with variations in these parameter(s): header pins soldered? bulk packaged? Select variant...

Compare all products in A4988 Stepper Motor Driver Carriers.

Description | Specs (12) | Pictures (8) | Resources (8) | FAQs (4) | On the blog (4)

Dimensions

Size:	0.6" × 0.8"
Weight:	1.3 g[1]

General specifications

Minimum operating voltage:	8 V
Maximum operating voltage:	35 V
Continuous current per phase:	1 A[2]
Maximum current per phase:	2 A[3]
Minimum logic voltage:	3 V
Maximum logic voltage:	5.5 V
Microstep resolutions:	full, 1/2, 1/4, 1/8, and 1/16
Reverse voltage protection?:	N
Bulk packaged?:	N
Header pins soldered?:	N[4]

8.8 DATA SHEETS FOR ELECTRICAL COMPONENTS

LM339 Comparator
LM339 Comparator Datasheet: [Online] Available: http://www.ti.com/lit/ds/symlink/lm339.pdf
Accessed: January 29th, 2019.

TEXAS INSTRUMENTS

LM139, LM239, LM339, LM139A
LM239A, LM339A, LM2901, LM2901AV, LM2901V
SLCS006U – OCTOBER 1979 – REVISED NOVEMBER 2018

LM339, LM239, LM139, LM2901 Quad Differential Comparators

1 Features

- Wide Supply Ranges
  - Single Supply: 2 V to 36 V (Tested to 30 V for Non-V Devices and 32 V for V-Suffix Devices)
  - Dual Supplies: ±1 V to ±18 V (Tested to ±15 V for Non-V Devices and ±16 V for V-Suffix Devices)
- Low Supply-Current Drain Independent of Supply Voltage: 0.8 mA (Typical)
- Low Input Bias Current: 25 nA (Typical)
- Low Input Offset Current: 3 nA (Typical) (LM139)
- Low Input Offset Voltage: 2 mV (Typical)
- Common-Mode Input Voltage Range Includes Ground
- Differential Input Voltage Range Equal to Maximum-Rated Supply Voltage: ±36 V
- Low Output Saturation Voltage
- Output Compatible With TTL, MOS, and CMOS
- On Products Compliant to MIL-PRF-38535, All Parameters Are Tested Unless Otherwise Noted. On All Other Products, Production Processing Does Not Necessarily Include Testing of All Parameters.

2 Applications

- Industrial
- Automotive
  - Infotainment and Clusters
  - Body Control Modules
- Power Supervision
- Oscillators
- Peak Detectors
- Logic Voltage Translation

3 Description

The LMx39x and the LM2901x devices consist of four independent voltage comparators that are designed to operate from a single power supply over a wide range of voltages. Operation from dual supplies also is possible, as long as the difference between the two supplies is 2 V to 36 V, and V_{CC} is at least 1.5 V more positive than the input common-mode voltage. Current drain is independent of the supply voltage. The outputs can be connected to other open-collector outputs to achieve wired-AND relationships.

The LM139 and LM139A devices are characterized for operation over the full military temperature range of –55°C to +125°C. The LM239 and LM239A devices are characterized for operation from –25°C to +85°C. The LM339 and LM339A devices are characterized for operation from 0°C to 70°C. The LM2901, LM2901AV, and LM2901V devices are characterized for operation from –40°C to +125°C.

Device Information(1)

PART NUMBER	PACKAGE	BODY SIZE (NOM)
LM139x	CDIP (14)	21.30 mm × 7.60 mm
	LCCC (20)	8.90 mm × 8.90 mm
	CFP (14)	9.20 mm × 6.29 mm
LM139x, LM239x, LM339x, LM2901x	SOIC (14)	8.70 mm × 3.90 mm
LM239, LM339x, LM2901	PDIP (14)	19.30 mm × 6.40 mm
LM239, LM2901	TSSOP (14)	5.00 mm × 4.40 mm
LM339x, LM2901	SO (14)	10.20 mm × 5.30 mm
LM339x	SSOP (14)	6.50 mm × 5.30 mm

(1) For all available packages, see the orderable addendum at the end of the data sheet.

Simplified Schematic

LM7805 Voltage Regulator
LM7805 Voltage Regulator Datasheet: [Online] Available: https://www.sparkfun.com/datasheets/Components/LM7805.pdfAccessed: January 29th, 2019.

recommended operating conditions

			MIN	MAX	UNIT
V_I	Input voltage	μA7805C	7	25	V
		μA7808C	10.5	25	
		μA7810C	12.5	28	
		μA7812C	14.5	30	
		μA7815C	17.5	30	
		μA7824C	27	38	
I_O	Output current			1.5	A
T_J	Operating virtual junction temperature	μA7800C series	0	125	°C

electrical characteristics at specified virtual junction temperature, V_I = 10 V, I_O = 500 mA (unless otherwise noted)

PARAMETER	TEST CONDITIONS	T_J†	μA7805C			UNIT
			MIN	TYP	MAX	
Output voltage	I_O = 5 mA to 1 A, V_I = 7 V to 20 V, $P_D \le 15$ W	25°C	4.8	5	5.2	V
		0°C to 125°C	4.75		5.25	
Input voltage regulation	V_I = 7 V to 25 V	25°C		3	100	mV
	V_I = 8 V to 12 V			1	50	
Ripple rejection	V_I = 8 V to 18 V, f = 120 Hz	0°C to 125°C	62	78		dB
Output voltage regulation	I_O = 5 mA to 1.5 A	25°C		15	100	mV
	I_O = 250 mA to 750 mA			5	50	
Output resistance	f = 1 kHz	0°C to 125°C		0.017		Ω
Temperature coefficient of output voltage	I_O = 5 mA	0°C to 125°C		−1.1		mV/°C
Output noise voltage	f = 10 Hz to 100 kHz	25°C		40		μV
Dropout voltage	I_O = 1 A	25°C		2		V
Bias current		25°C		4.2	8	mA
Bias current change	V_I = 7 V to 25 V	0°C to 125°C			1.3	mA
	I_O = 5 mA to 1 A				0.5	
Short-circuit output current		25°C		750		mA
Peak output current		25°C		2.2		A

† Pulse-testing techniques maintain the junction temperature as close to the ambient temperature as possible. Thermal effects must be taken into account separately. All characteristics are measured with a 0.33-μF capacitor across the input and a 0.1-μF capacitor across the output.

Transistors
TIP147/2 Datasheet: [Online] Available: https://www.st.com/content/ccc/resource/technical/document/datasheet/ec/61/1c/fd/4c/fe/48/b5/CD00000914.pdf/files/CD00000914.pdf/jcr:content/translations/en.CD00000914.pdf Accessed: January 29th, 2019.

1 Absolute maximum ratings

Table 2. Absolute maximum ratings

Symbol	Parameter	Value	Unit
V_{CBO}	Collector-base voltage ($I_E = 0$)	100	V
V_{CEO}	Collector-emitter voltage ($I_B = 0$)	100	V
V_{EBO}	Emitter-base voltage ($I_C = 0$)	5	V
I_C	Collector current	10	A
I_{CM}	Collector peak current	20	A
I_B	Base current	0.5	A
P_{TOT}	Total dissipation at $T_{case} = 25$ °C	125	W
T_{STG}	Storage temperature	-65 to 150	°C
T_J	Max. operating junction temperature	150	°C

Note: For PNP type voltage and current are negative.

Table 3. Thermal data

Symbol	Parameter		Value	Unit
R_{thJC}	Thermal resistance junction-case	max	1	°C/W

Diodes
[]: IN4001 Datasheet: [Online] Available: https://www.vishay.com/docs/88503/1n4001.pdf Accessed: January 29th, 2019.

VISHAY

1N4001 thru 1N4007

Vishay General Semiconductor

General Purpose Plastic Rectifier

DO-204AL (DO-41)

FEATURES

- Low forward voltage drop
- Low leakage current
- High forward surge capability
- Solder dip 275 °C max. 10 s, per JESD 22-B106
- Compliant to RoHS Directive 2002/95/EC and in accordance to WEEE 2002/96/EC

Pb e3 RoHS COMPLIANT

TYPICAL APPLICATIONS

For use in general purpose rectification of power supplies, inverters, converters and freewheeling diodes application.

Note

- These devices are not AEC-Q101 qualified.

PRIMARY CHARACTERISTICS	
$I_{F(AV)}$	1.0 A
V_{RRM}	50 V to 1000 V
I_{FSM} (8.3 ms sine-wave)	30 A
I_{FSM} (square wave t_p = 1 ms)	45 A
V_F	1.1 V
I_R	5.0 µA
T_J max.	150 °C

MECHANICAL DATA

Case: DO-204AL, molded epoxy body
Molding compound meets UL 94 V-0 flammability rating
Base P/N-E3 - RoHS compliant, commercial grade

Terminals: Matte tin plated leads, solderable per J-STD-002 and JESD 22-B102
E3 suffix meets JESD 201 class 1A whisker test

Polarity: Color band denotes cathode end

MAXIMUM RATINGS (T_A = 25 °C unless otherwise noted)

PARAMETER		SYMBOL	1N4001	1N4002	1N4003	1N4004	1N4005	1N4006	1N4007	UNIT
Maximum repetitive peak reverse voltage		V_{RRM}	50	100	200	400	600	800	1000	V
Maximum RMS voltage		V_{RMS}	35	70	140	280	420	560	700	V
Maximum DC blocking voltage		V_{DC}	50	100	200	400	600	800	1000	V
Maximum average forward rectified current 0.375" (9.5 mm) lead length at T_A = 75 °C		$I_{F(AV)}$	1.0							A
Peak forward surge current 8.3 ms single half sine-wave superimposed on rated load		I_{FSM}	30							A
Non-repetitive peak forward surge current square waveform T_A = 25 °C (fig. 3)	t_p = 1 ms	I_{FSM}	45							A
	t_p = 2 ms		35							
	t_p = 5 ms		30							
Maximum full load reverse current, full cycle average 0.375" (9.5 mm) lead length T_L = 75 °C		$I_{R(AV)}$	30							µA
Rating for fusing (t < 8.3 ms)		I^2t [1]	3.7							A^2s
Operating junction and storage temperature range		T_J, T_{STG}	- 50 to + 150							°C

Note

[1] For device using on bridge rectifier appliaction